ZNO NANOPARTICLES AS SATURABLE ABSORBER FOR PASSIVELY Q-SWITCHED FIBER LASER IN C-AND S-BAND

CHERRIE LEE SUE JING

INSTITUTE OF GRADUATE STUDIES
UNIVERSITY OF MALAYA
KUALA LUMPUR

2018

ZNO NANOPARTICLES AS SATURABLE ABSORBER FOR PASSIVELY Q-SWITCHED FIBER LASER IN C-AND S-BAND

CHERRIE LEE SUE JING

DISSERTATION SUBMITTED IN FULFILMENT OF THE REQUIREMENTS FOR THE DEGREE OF MASTER OF PHILOSOPHY

INSTITUTE OF GRADUATE STUDIES
UNIVERSITY OF MALAYA
KUALA LUMPUR

2018

UNIVERSITY OF MALAYA

ORIGINAL LITERARY WORK DECLARATION

Name of Candidate: Cherrie Lee Sue Jing

Matric No: HGG150001

Name of Degree: Master of Philosophy (Photonics)

Title of Dissertation: ZnO Nanoparticles as Saturable Absorber for Passively Q-Switched Fiber Laser in C-and S-band.

Field of Study: Photonics

I do solemnly and sincerely declare that:

(1) I am the sole author/writer of this Work;
(2) This Work is original;
(3) Any use of any work in which copyright exists was done by way of fair dealing and for permitted purposes and any excerpt or extract from, or reference to or reproduction of any copyright work has been disclosed expressly and sufficiently and the title of the Work and its authorship have been acknowledged in this Work;
(4) I do not have any actual knowledge nor do I ought reasonably to know that the making of this work constitutes an infringement of any copyright work;
(5) I hereby assign all and every rights in the copyright to this Work to the University of Malaya ("UM"), who henceforth shall be owner of the copyright in this Work and that any reproduction or use in any form or by any means whatsoever is prohibited without the written consent of UM having been first had and obtained;
(6) I am fully aware that if in the course of making this Work I have infringed any copyright whether intentionally or otherwise, I may be subject to legal action or any other action as may be determined by UM.

Candidate's Signature   Date:

Subscribed and solemnly declared before,

Witness's Signature   Date:

Name:

Designation:

ZNO NANOPARTICLES AS SATURABLE ABSORBER FOR PASSIVELY Q-SWITCHED FIBER LASER IN C-AND S-BAND

ABSTRACT

This work investigates the characteristics of pulses generated via passive Q-switching in S- and C-band using zinc oxide nanoparticles as saturable absorber. Unlike active Q-switching, passive Q-switching is a cheaper and simpler alternative to obtain pulses with repetition rates in the range of kilohertz and pulse width of mircoseconds. There are several techniques to obtain passively Q-switched laser such as the employment of nonlinear polarization rotation (NPR), semiconductor saturable absorber (SESAM), carbon-based saturable absorber (single-walled carbon nanotubes (SWCNT), graphene and graphene oxide) and transition metal-dichalcogenides saturable absorber (molybdenum disulfide, molybdenum diselenide, tungsten disulfide and tungsten diselenide). Nanomaterials such as zinc oxide nanoparticles have distinctive optical, electronic and mechanical properties which made them a suitable candidate as a saturable absorber (SA) for passively Q-switched laser. Erbium-doped fiber (EDF) is used as the gain medium in the laser cavity to obtain Q-switched pulses in C-band. C-band is the most commonly used wavelength in optical communications. Due to increasing data traffic, there is a demand to expand the optical network to other bands to reduce network congestion. One of the bands being considered to accommodate this expansion is S-band. Depressed-cladding erbium-doped fiber (DC-EDF) is used as the gain medium in the laser cavity to obtain Q-switched pulses in S-band. The tuning range of these pulses in C-band and S-band are also investigated. The results obtained from this work is instrumental as Q-switched lasers are widely used in many applications such as aesthetic treatment, biomedical diagnostic, remote-sensing and telecommunications.

Keywords: Q-switching, Fiber Laser, Tunable laser, Nanomaterials, Zinc oxide

NANOPARTIKEL ZINK OKSIDA SEBAGAI PENYERAP BOLEH-TEPU UNTUK LASER Q-SWITCHED DALAM JALUR-C DAN -S

ABSTRAK

Penyelidikan ini bertujuan untuk menyiasat ciri-ciri denyut *Q-switched* secara pasif dalam jalur-S dan -C menggunakan nanopartikel zink oksida sebagai penyerap boleh-tepu. Berbanding dengan kaedah *Q-switched* secara aktif, kaedah *Q-switched* secara pasif adalah lebih murah dan mudah untuk menghasilkan denyutan yang memiliki kadar repetisi dalam lingkungan kHz dan kelebaran denyut optik dalam lingkungan µs. Antara teknik dan cara-cara untuk mendapatkan denyut *Q-switched* secara pasif adalah menggunakan teknik putaran pengkutuban tak linear (NPR), penyerap boleh-tepu semikonduktor (SESAM), penyerap boleh-tepu berasaskan karbon (tiub nanokarbon berdinding tunggal (SWCNT), graphene dan graphene oksida) dan penyerap boleh-tepu logam peralihan-*dichalcogenides* (molybdenum diselenida, molybdenum disulfida, tungsten disulfida dan tungsten diselenida). Bahan nano seperti nanopartikel zink oksida memiliki ciri-ciri tersendiri dalam aspek optik, elektronik dan mekanik yang menjadikannya sesuai sebagai penyerap boleh-tepu untuk menghasilkan laser *Q-switched*. Gentian optik berdop erbium digunakan sebagai medium gandaan dalam rongga laser untuk menghasilkan denyutan dalam jalur-C. Jalur-C adalah jalur gelombang yang sering digunakan dalam kominukasi optik. Peningkatan trafik data mendorong keperluan untuk meluaskan rangkaian optik ke jalur yang lain untuk mengurangkan kesesakan rangkaian. Salah satu jalur yang dianggap sesuai untuk menampung kesesakan rangkaian ialah jalur-S. Gentian optik berdop erbium dengan rekabentuk pelapisan ditekan digunakan sebagai medium gandaan dalam rongga laser untuk menghasilkan denyut *Q-switched* dalam jalur-S. Julat pelarasan denyutan dalam jalur-C juga disiasat. Hasil kajian ini adalah penting kerana laser *Q-switched* sering digunakan dalam pelbagai

aplikasi seperti rawatan kecantikan, diagnostik bioperubatan, penderiaan jauh dan sistem telekomunikasi.

Kata kunci: Laser *Q-switched*, Laser Gentian Optik, Laser Boleh-Laras , Nanopartikel, Zink Oksida

ACKNOWLEDGEMENTS

I would like to express my gratitude to my main supervisor, Professor Ulung Datuk Dr. Harith Bin Ahmad for his excellent guidance throughout the entire process of this thesis. Not forgetting, my co-supervisor, Dr Mohd. Afiq Bin Ismail for initiating the idea and sharing his expertise in pulse lasers.

I would also like to thank my colleagues and staffs at Photonics Research Centre for their helpful assistance and support until the completion of this thesis.

TABLE OF CONTENTS

LIST OF FIGURES

LIST OF TABLES

LIST OF SYMBOLS AND ABBREVIATIONS

ASE	:	Amplified spontaneous emission
CNT	:	Carbon nanotube
DC-EDF	:	Depressed-cladding erbium-doped fiber
EDF	:	Erbium-doped fiber
FESEM	:	Field emission scanning electron microscope
NPR	:	Nonlinear polarization rotation
SA	:	Saturable absorber
SEM	:	Scanning electron microscope
SESAM	:	Semiconductor saturable absorber
SNR	:	Signal-to-noise ratio
SWCNT	:	Single-walled carbon nanotube
TI	:	Topological insulator
TMD	:	Transition metal dichalcogenides
UV	:	Ultraviolet
WDM	:	Wavelength division multiplexer
XRD	:	X-ray diffraction
ZnO	:	Zinc oxide

CHAPTER 1: INTRODUCTION

1.1 Background and Motivation

Remote sensing, biomedical diagnostics, aesthetic treatments, material processing and telecommunications are some of the few examples of applications of Q-switched lasers (Ursula Keller, 2003). Q-switching can be achieved via active or passive methods. In the case of active Q-switching, the loss in the laser's resonator is manipulated externally using modulators such as electro-optic or acousto-optic devices. However, in passive Q-switching, this loss is easily controlled using a saturable absorber. Passive Q-switching is generally a preferable choice than active Q-switching due to its simplicity and do not require additional electronics. Some of the examples of saturable absorbers that have been reported are semiconductor saturable absorber mirrors (SESAMs) (U. Keller et al., 1996) and carbon nanotubes (CNTs) (Zhou, Wei, Dong, & Liu, 2010). Nonlinear polarization (NPR) is also another method that can replicate the action of a saturable absorber. However, these saturable absorbers and technique have a few drawbacks such as narrow operating bandwidth, environmental sensitivity, delicate fabrication process or intricate optical alignments. So far, one of the most successful materials as saturable absorber is graphene due to its simple implementation into cavity design. ultrabroadband absorption and ultrafast recovery times (Bao et al., 2010). Special materials such as bismuth selenide (Be_2Se_3) and bismuth telluride (Be_2Te_3) (Hasan & Kane, 2010) or otherwise known as topological insulators (TIs) which allow electrons to conduct on its surface but acts as an insulator in its interior, have also been gaining popularity along with transition-metal dichalcogenides (TMDs) such as tungsten disulphide (WS_2) (H. Ahmad, N. E. Ruslan, et al., 2016) and molybdenum disulphide (MoS_2) (R. I. Woodward et al., 2014). These saturable absorber materials belong to a class of material called nanomaterials which exhibit properties that are unique and interesting, yet complementary to graphene (Q. H. Wang, Kalantar-Zadeh, Kis, Coleman, & Strano, 2012; R. I. Woodward, Howe, Hu, et al., 2015). Metal oxide nanostructures like titanium dioxide (TiO_2) nanoparticles and zinc oxide (ZnO) nanoparticles belong to this class of material. TiO_2 as saturable absorber for passive Q-switching has been demonstrated (H. Ahmad, Siti Aisyah Reduan, et al., 2016) and the results are as good as conventional saturable absorbers. Other than TiO_2, there are not many studies on metal oxide as potential saturable absorbers. Before the publication of this work, ZnO as saturable absorber for passive Q-switching had yet to be reported.

ZnO exhibits many saturable absorption properties. When probed using time-resolved second harmonic generation technique, ZnO has a fast recovery time of 1-5 ps (Johnson et al., 2004), which implies that short pulse in the picosecond range is possible using ZnO as saturable absorber. Moreover, ZnO possess high third-order nonlinear coefficient (Petrov et al., 2003). Single beam z-scan technique was performed to measure the nonlinearity and revealed that the nonlinear absorption is attributed to the two-photon resonance to the band edge and exciton energy level whereas the optical nonlinearity is attributed to the free-carrier effect in ZnO (Lin, Chen, Lin, & Hsieh, 2005). Due to its large binding energy of 60 meV and very wide bandgap of 3.37 eV which corresponds to 368 nm in wavelength (Z. L. Wang, 2004), ZnO nanostructures are used extensively in optoelectronic devices such as laser diodes, light emitting diodes and photodetectors especially for UV range applications (Soci et al., 2007; Ümit, Hofstetter, & Morkoc, 2010).

Conventional band (C-band) as the name suggests is the most common wavelength used in optical telecommunications. C-band comprises of wavelength region of 1530-1563 nm and Q-switched pulses at this region are usually achieved using erbium-doped fiber (EDF) as the gain medium. However, to accommodate the expansion of data traffic. Other wavelength bands are currently being explored. One of them is S-band, which encompasses a wavelength range of 1460-1530 nm. A few studies had been done on pulse laser in S-band which utilized depressed-cladding erbium-doped fiber (DC-EDF) laser as the gain medium (H Ahmad et al., 2017; Harun, Dimyati, Jayapalan, & Ahmad, 2007). The characteristics of Q-switched pulse in C-band and S-band using ZnO nanoparticles as saturable absorber were investigated in this work.

1.2 Scope of Research and Research Objectives

This research focusses on Q-switching in the region of C-band (1530-1563 nm) and in the region of S-band (1460-1530 nm). EDF was used as the gain medium to generate Q-switched pulses in the C-band while DC-EDF was used as the gain medium to generate Q-switched pulses in the S-band. Another alternative band worth exploring is the L-band (1560 -1630 nm). However, due to lack of components, this work will only focus on C- and S-band. Both wavelength bands were pumped by a 974 nm laser diode and utilized ZnO as the saturable absorber. The optical properties of ZnO as saturable absorber such as saturation intensity and modulation depth were also characterized and compared to other existing saturable absorbers. The performances of the Q-switched lasers using the ZnO saturable absorber were also investigated.

The objectives of this work are listed as follow:

i. To study the optical properties of ZnO nanoparticles as saturable absorber by characterizing its nonlinear optical absorption. This includes measurements of the modulation depth and saturation intensity using the balanced twin detector system.

ii. To explore the possibility of ZnO as saturable absorber for passive Q-switching in C- and S-band. The configuration of each of the laser cavities are designed and modified to obtain stable Q-switched pulse in C-band and S-band.

iii. To analyze the characteristics of the Q-switched pulses in C-band and S-band by measuring and calculating the repetition rate, pulse width, peak power, pulse energy and signal-to-noise ratio.

iv. To investigate the tuning range of the Q-switched pulse using ZnO in C-band and S-band.

1.3 Importance and Relevance of Research

One of the main motivations of this study is the lack of studies on metal oxides as saturable absorber, particularly ZnO. The possibility of ZnO as saturable absorber will open a large group of other metal oxides to be explored as saturable absorber. This will provide a wide option of saturable absorber since different saturable absorbers with their own distinct characteristics could be used for different needs.

The study of the tunability of the Q-switched laser is important as this feature is widely used in wavelength division multiplexing (WDM) technology, biomedical research, spectroscopy and telecommunications. This could potentially replace SESAM as the dominant saturable absorber since one of the major concerns about SESAMs is their limited tuning range.

Two wavelengths bands were investigated in this research: C-band and S-band. Despite being the most commonly used band, the capacity of C-band is not infinite. To fulfil the demand of increasing data traffic, S-band is now explored to accommodate this expansion. This research could be extended to obtain supercontinuum and mode-locked laser which are used in a vast number of applications. The outcomes of this research will benefit the advancement of telecommunication, biomedicine, material processing and many other fields which require lasers.

1.4 Dissertation Overview

This dissertation begins with Chapter 1 which introduces the motivation, objectives, importance and relevance of this work.

Chapter 2 provides the theoretical concepts about pulse laser, with emphasis on passive Q-switching. The role of a saturable absorber is discussed, and state-of-the-art saturable absorbers are also introduced.

The fabrication of the zinc oxide saturable absorber is explained in Chapter 3. Material characterization and optical characterization of the saturable absorber are also described and presented in this chapter to give a concise description of the saturable absorber before being introduced again as a material used in Chapter 4.

Chapter 4 describes the experimental setups that are used to obtain Q-switching in C-band and S-band using the ZnO SA. The types of instruments used to obtain all the necessary measurements are also listed.

Important results and discussions are presented in Chapter 5 before the dissertation ends with conclusion and future outlook of this work.

CHAPTER 2: LITERATURE REVIEW

2.1 Principles of Laser

Laser is an acronym for Light Amplified Stimulated Emission Radiation. As the name suggests, the main principle behind laser operation is stimulated emission. Nevertheless, photons undergo three types of interactions: absorption, spontaneous emission and stimulated emission, as illustrated in Figure 2.1. Only stimulated emission will lead to laser operation. In absorption, electron in the ground state absorbs energy from a photon to jump to a higher energy level. In spontaneous emission, electron in the higher energy state returns to a lower energy state by emitting a photon. Electron in the higher state has a very short lifetime, and therefore, excited electron only remained on the upper state for a very short duration before spontaneously returns to the lower state. As this process occur spontaneously, the photons emitted are not in phase or in other words, incoherent. Unlike spontaneous emission, stimulated emission is not a natural process. Incident photons supply the energy to force the electrons in the upper state to return to the lower state. As a result, two photons are emitted in this process, one due to the incident photon and the other due to the energy released when the excited electron returns to the lower energy level. All photons emitted via stimulated emission are coherent as they are all in phase, have the same frequency and energy (Svelto, 2010).

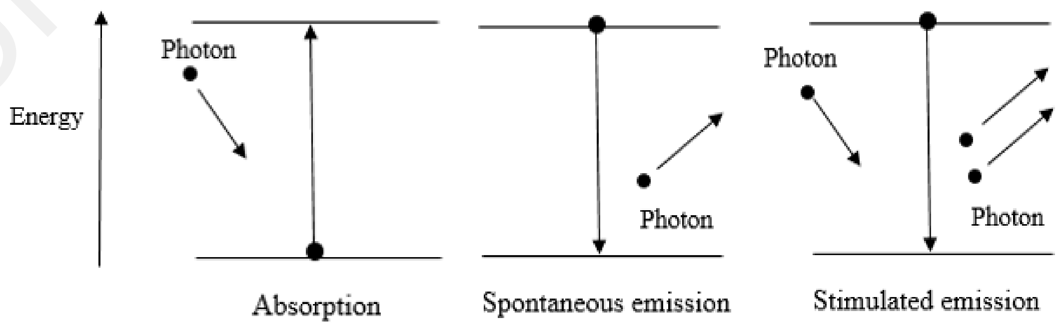

Figure 2.1: Mechanism of absorption, spontaneous emission and stimulated emission.

To amplify light for laser operation, population inversion is required, whereby the population of electrons in the higher energy state is higher than the population of electrons in the lower energy state. This typically cannot be achieved in a two-energy level system as the population of electrons in the lower state is always greater than the population of electrons in the upper energy level. Population inversion can be achieved using 3 or higher number of energy levels. The mechanism of a 3-level system is illustrated in Figure 2.2.

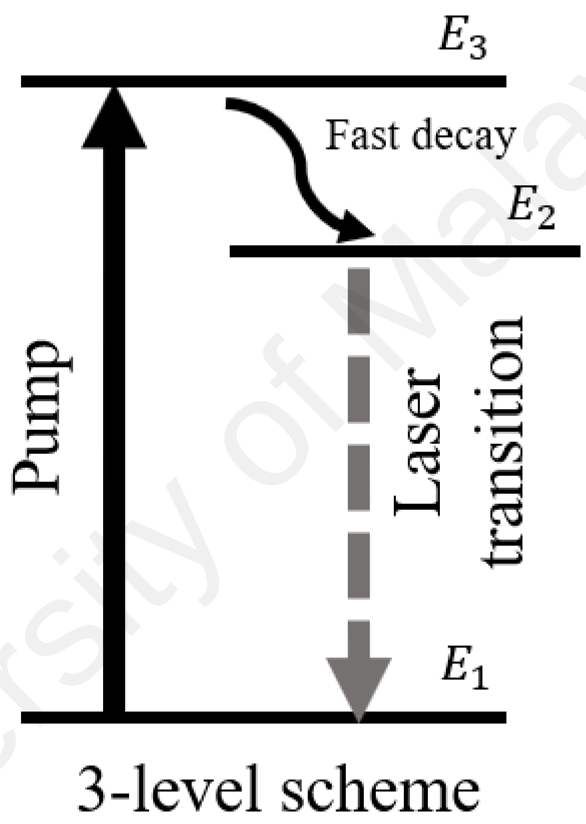

Figure 2.2: The mechanism of a 3-level system in laser.

Electrons at the lowest energy level (E_1) are pumped to the highest energy level (E_3). But due to the relative short lifetime at E_3, most of the electrons are quickly demoted to a lower energy level (E_2). At this energy level, the lifetime is relatively much longer, thus, a large number of electrons are accumulated at this energy level, allowing population inversion to occur. Initially, the electron decays from E_2 to E_1 via spontaneous emission. When a photon emitted via this process matches the energy difference between E_2 and E_1, this particular photon will stimulate the decay of an electron from E_2 to E_1. It is this transition that contributes to typical laser operation.

2.1.1 Gain Medium

A typical laser system consists of a pump source, an amplifying gain medium and an optical feedback cavity. The gain medium is pumped by the pump source to build up the population inversion. When the population inversion grows to a certain threshold value, photons are emitted via stimulated emission. These photons oscillate in the optical cavity and continue to grow until a steady state is attained. It will eventually reach a state whereby the stimulated emission is more dominant than the pump. At this point, the population inversion starts to decrease as there are more electrons decaying to lower level than the number of electrons pumped to a higher energy level. When the population inversion reduces to a certain critical value, the emitted photons will reduce as well. At this point, the pumping process becomes dominant again and a new cycle begins (Svelto, 2010).

2.1.1.1 Erbium-Doped Fiber

Erbium-doped fiber (EDF) is widely used as the gain medium for amplification around 1550 nm wavelength (located within the C-band region) in ring laser cavity configuration. The first laser using erbium-doped glass was demonstrated in 1965 by Snitzer (Snitzer & Woodcock, 1965). EDF laser is a 3-level system whereby the Er^{3+} ions are pumped by light in 980 nm wavelength. When the excited electrons return to the ground state, photons at a longer wavelength, 1550 nm are emitted. The emission of the laser in the optical communication network window, lead to the development of EDF amplifier as the replacement of conventional electronic regenerator in communication systems (Becker, Olsson, & Simpson, 1999).

2.1.1.2 Depressed-Cladding Erbium-Doped Fiber

By looking at the current growth of data traffic, the 33 nm window in optical communication C-band (1530-1563 nm) will soon be insufficient to support current trend of data usage. In order to cope with the increasing demand of bandwidth, one possibility worth exploring is the expansion of the existing C-band to other band regions such as short-band or also known as S-band, covering wavelength range of 1460 to 1530 nm. The amplification of standard EDF is limited to C- and L-band (1530 -1563 nm and 1560 – 1620 nm). To achieve amplification in S-band (1460 -1530 nm), other techniques which are commonly employed are the use of Raman amplifier, thulium-doped fiber amplifier and semiconductor optical amplifier. Although these traditional techniques produce amplification with notable gain and low noise, their disadvantages (when compared to EDF amplifiers) in terms of complexity, incompatibility and high-cost, greatly outweigh their advantages (Arbore, Zhou, Keaton, & Kane, 2002; Zulkifli, Jemangin, Harun, & Ahmad, 2011). A better alternative was published by Arbore et.al (Arbore et al., 2002) which employed the use of depressed-cladding erbium-doped fiber (DC-EDF) for amplification in S-band. This approach has the advantages of EDF and at the same time maintaining similar gain achieved by traditional methods. Due to its distinctive refractive index profile, depressed-cladding erbium-doped fiber suppresses amplified spontaneous emission (ASE) at higher wavelengths (C- and L-band) and consequently, enable the ASE to boost at shorter wavelength regime (S-band). The study of signal transmission in S-band is crucial, especially in the field of telecommunications whereby the dominant operating wavelength is C-band. The bandwidth of C-band is limited, hence, other wavelength bands such as S-band is worth exploring to accommodate the current heavy data traffic in C-band.

2.2 Principles of Q-Switching

Q-switching is a technique of producing short, intense pulses of light by modulating the resonator loss of the laser cavity. The resonator loss is quantified as the quality factor (Q-factor). A small Q-factor indicates that the resonator loss is high whereas a high Q-factor signifies that the resonator loss is low. When a shutter is introduced into the cavity, lasing action is prevented (Q-factor is low). Meanwhile, the gain medium is continuously pumped whereas the stimulated emission process which generate the cavity photons is prohibited. Consequently, the population inversion could reach a much higher value than its original threshold value (without the presence of the shutter). When this shutter is opened, stimulated emission is no longer prohibited and starts to deplete the population inversion and the cavity photons increases very quickly. The Q-factor is high at this stage. The cavity photon number reaches its maximum peak value and the population inversion decreases to below its threshold value. The accumulated energy is released as short intense light pulse in the range of a few nanoseconds. The switch from a low Q to a high Q to produce such pulse laser, gave this phenomenon the name Q-switching.

The quality of the Q-switched pulse can be characterized by its signal-to-noise ratio (SNR), pulse duration (t_p), repetition rate (f_r), pulse energy (E_p) and peak power (P_p). Typically, the repetition rate of Q-switched pulse is in the order of kilohertz and has pulse duration in the order of microseconds. The pulse energy is calculated using this relation:

$$E_p = \frac{P_{av}}{f_r} \qquad 2.1$$

where P_{av} is the average power measured using a power meter. The peak power is related to the pulse energy as follow (Koechner, 2006):

$$P_p = \frac{E_p}{t_p} \qquad 2.2$$

2.2.1 Methods of Q-Switching

There are two types of Q-switching: active and passive. Active Q-switching requires mechanical action such as the use of electro-optic or acousto-optic devices as Q-switcher to modulate the loss of the cavity.

Electro-optical Q-switching is based on Pockel's effect. Nonlinear crystals such as lithium tantalate (El-Sherif & King, 2003) experience changes in their refractive indices when voltage is applied, altering the plane of polarization of propagating light. The change of plane of polarization will reduce the growth of cavity photons and hence reduce the Q-factor of the cavity. When the voltage is removed, the plane of polarization returns to normal and the Q-factor increases, producing a laser pulse.

Acousto-optical Q-switching manipulates the refractive index of the material by using piezoelectric transducer which generates strain that changes the refractive index of the material. Typical material used as acousto-optic modulators are fused quartz, germanium and cadmium (Antipov, Eranov, & Kositsyn, 2016). The sound wave generated by the transducer changes the refractive index of the material periodically, operating like an optical grating which diffracts light from the incident beam, creating loss in the resonator. When the transducer is switched off, light can pass through without hindrance and the cavity returns to high Q.

In contrast, all these external mechanical actions are not required in passive Q-switching whereby the switching ability is done within the saturable absorber. This is the biggest advantage of passive Q-switching over active Q-switching.

2.3 Saturable Absorbers in Passive Q-Switching

A saturable absorber has the ability to vary the loss in the resonator depending on the intensity of the incident light. Incident light with high intensity is able to saturate the saturable absorber, reducing the resonator loss temporarily (high Q) while incident light with weak intensity is unable to saturate the saturable absorber and will therefore, experience a greater loss. When the saturable absorber is integrated into a laser cavity, the incident photon is absorbed by the saturable absorber, making the Q-factor of the cavity low while population inversion starts to accumulate. As the intensity of light passing through the saturable absorber increases, more and more electrons in the saturable absorber are in the excited state until it reaches a saturation point when all the electrons in the saturable absorber's ground state are depleted. When the saturable absorber is saturated, the absorber is said to be bleached or in other word, transparent to the wavelength of the incident light, thus, increasing the Q-factor of the cavity (Svelto, 2010). This property of saturable absorber eliminates the need of complex mechanical switching devices to manipulate the cavity loses, making it easier and simpler to be integrated in a laser cavity.

2.3.1 Saturable Absorption Parameters

Saturable absorbers can be characterised by parameters such as modulation depth, non-saturable absorption, saturation intensity, recovery times and absorption bandwidth. The saturable absorption can be modelled by equation 2.3 (Garmire, 2000).

$$\alpha(I) = \frac{\alpha_0}{1 + \frac{I}{I_s}} + \alpha_{ns} \qquad 2.3$$

where I is the incident light intensity, I_s is the saturation intensity, α_0 is the modulation depth and α_{ns} is the non-saturable loss.

The modulation depth (α_0) can be measured using power-dependent absorption measurements. An optical pulse source is transmitted passing through the saturable absorber. This will induce a change of intensity at the output. The maximum change in the induced optical loss is defined as the modulation depth. The non-saturable loss (α_{ns})

is the loss that cannot be saturated by the saturable absorber due to non-saturable defect absorption, scattering loss, free-carrier absorption and many more. The intensity needed to lower the absorption to half of its unsaturated value in steady state is the saturation intensity (I_s). When the incident light has intensity lower than I_s, the optical absorption is large, preventing lasing to occur. On the other hand, when the incident light has intensity higher than I_s, the absorption is saturated, and the resonator loss suddenly becomes low, resulting in a high Q value for Q-switching to occur.

Recovery time is the time duration for a saturable absorber to return to its initial state from its excited state. For Q-switching, the recovery time of a saturable absorber is ideally longer than the pulse duration of the laser but shorter than the upper-state lifetime of the gain medium to prevent the resonator to lase prematurely (R. Paschotta). When selecting suitable types of saturable absorbers, these parameters need to be considered.

2.3.2 Types of Saturable Absorbers

There are many types of saturable absorbers. One of the earliest saturable absorber for passive q-switching is semiconductor saturable absorber mirrors (SESAMs) (R Paschotta et al., 1999). SESAM is made up of a semiconductor quantum well and a Bragg mirror. The operation wavelength can be varied from 400 nm up to 2500 nm by varying the type of semiconductor. In addition, SESAM offers flexibilities in terms of recovery times and saturation fluence. By varying the growth parameters during the fabrication of SESAM, these properties can be engineered to specific needs (Ursula Keller, 2007), which made SESAM the most commercially used saturable absorber. However, SESAM has some limitations. The fabrication process of SESAM is complex, time-consuming and expensive, creating a need to search for better saturable absorber alternatives.

Recent emerging saturable absorbers are nanomaterials. Nanomaterial-based saturable absorbers are compact, economical and robust (R. Woodward & Kelleher, 2015). The current popularity of nanomaterial-based SA was triggered by the discovery of graphene in 2004 (Novoselov et al., 2004). Many works using graphene as saturable absorber have been reported. The first demonstration of graphene as saturable absorber was demonstrated in 2011 (Bao et al., 2011) for passive mode-locking generating pulse of 1.23 ps. Monolayer graphene has a fast recovery time of 100-150 fs and slow recovery time of 405-570 fs. The ultrafast carrier dynamics coupled with its ultrabroadband absorption made graphene an ideal saturable absorber.

Besides graphene, another carbon allotrope that is used as saturable absorber is carbon nanotubes (CNTs) and often visualized as the tube version of rolled-up graphene. By manipulating the diameter, chirality and thickness of the tubes, the operating wavelength, bandwidth and modulation depth can be varied (Sobon et al., 2017; Shinji Yamashita, 2012). CNT as saturable absorber has been widely studied and reported (Martinez & Sun, 2013; Scardaci et al., 2008; S Yamashita et al., 2004).

Other interesting groups of saturable absorbers that are currently explored are topological insulators, transition metal dichalcogenides (TMDs) and black phosphorus. Topological insulator exhibits interesting properties whereby electrons conduct on its surface whereas the interior is an insulator. Examples of such materials are bismuth telluride (Be_2Te_3) and bismuth selenide (Be_2Se_3) (Chen et al., 2014; Luo et al., 2013; Yu et al., 2013). TMD has stoichiometry of MX_2, where M is a transition metal and X is a chalcogen. TMDs can be metallic or semiconducting depending on the type of transition metal and oxidation state. Semiconducting TMDs such as $MoSe_2$, MoS_2, WSe_2 and WS_2 are widely used for photonics applications (Mohanraj, Velmurugan, & Sivabalan, 2016) and particularly as saturable absorbers for passive Q-switching (H. Ahmad, N. E. Ruslan, et al., 2016; B. Chen et al., 2015; Huang et al., 2014; R. I. Woodward, Howe, Runcorn, et al., 2015). Black phosphorus has layer-dependent band gap (Tran, Soklaski, Liang, &

Yang, 2014), fulfilling the void between semi-metallic graphene and wide band gap TMDs. Using mechanical exfoliation method, black phosphorus can be easily fabricated and used as saturable absorber to generate Q-switched pulses (Y. Chen et al., 2015).

Nonetheless, not much attention has been focused on other types of nanomaterial as saturable absorber. Our group recently demonstrated passive Q-switching using TiO_2 nanoparticles (H. Ahmad, Siti Aisyah Reduan, et al., 2016) and silver nanoparticles (H Ahmad et al., 2016) as saturable absorbers. Other than that, zinc oxide nanoparticles as saturable absorber for passive Q-switching had yet to be reported.

2.3.3 Zinc Oxide Saturable Absorber

Zinc oxide is a semiconductor with a wide band gap of 3.37 eV (~ 368 nm) and large binding energy of 60 meV (Z. L. Wang, 2004). Due to its large band gap, ZnO is widely used in optoelectronics devices such as laser diode, light-emitting diodes and photodetectors (Soci et al., 2007; Ümit et al., 2010). In terms of its ultrafast carrier dynamics, zinc oxide exhibits a fast (1-5 ps) and a slow component (>50 ps) recovery time when examined using time-resolved second-harmonic generation. The slow component corresponds to free exciton decay whereas the fast component is accounted by stimulated emission either via exciton-exciton or electron-hole plasma recombination (Johnson et al., 2004). Moreover, zinc oxide has high third order nonlinearity (Petrov et al., 2003). The nonlinearity was measured using single beam z-scan technique and revealed that the nonlinear absorption is correlated to the two-photon resonance to the band edge and exciton energy level whereas the optical nonlinearity is attributed to the free-carrier effect in ZnO (Lin et al., 2005). The short recovery time and optical nonlinearity present in ZnO contribute to zinc oxide suitability as saturable absorber.

CHAPTER 3: FABRICATION AND CHARACTERIZATION OF ZNO SATURABLE ABSORBER

3.1 Introduction

The focus of this chapter is to describe the process and methods used to prepare the zinc oxide nanoparticles saturable absorber and the subsequent characterizations. ZnO can be synthesized by chemical methods such as precipitation (L. Wang & Muhammed, 1999) and sol-gel technique (Westin & Nygren, 1992) or by physical methods such as gas evaporation (El-Shall, Graiver, Pernisz, & Baraton, 1995). This is often accompanied by characterizations such as field emission scanning electron microscopy (FESEM) to determine the particle size, and x-ray diffraction.

Optical characterizations such as the absorption spectrum and modulation depth were also measured to investigate the nonlinear optical absorption properties of the zinc oxide as a saturable absorber.

3.2 Preparation and Characterizations of Zinc Oxide Saturable Absorber

For this work, the saturable absorber (ZnO) was prepared using zinc oxide nanoparticles obtained from Sigma Aldrich Malaysia Sdn Bhd and used without further purification. The process of developing the thin film containing zinc oxide was done by Z. A. Ali from the Corrosion and Coating Laboratory at the Department of Physics, University of Malaya.

The zinc oxide nanoparticles were originally in powder form. To integrate the saturable absorber into the laser cavity, the most feasible and least complicated way is to embed the zinc oxide in to a thin film. That way, the thin film containing the nanoparticles can be attached to the end of the fiber ferrules using index-matching gel, creating a fiber-compatible saturable absorber. The thin film was developed by mixing the zinc oxide powder (5 wt%) into a mixture of silane and ethanol. The silane and ethanol mixture had a weight ratio of 1:1. The mixture was ultrasonicated for half an hour. After that, sulfuric acid (10 wt%) was added and then ultrasonicated for another 5 minutes. The resulting mixture was poured into a plastic mold and left to dry for 3 days under room temperature. The fabricated thin film of zinc oxide has a thickness of 0.15±0.1 mm. Similar fabrication technique has also been reported by (H Ahmad et al., 2016) using silver nanoparticles.

3.2.1 Field Emission Scanning Electron Microscopy

Microscopic image of the ZnO nanoparticles was taken using field emission scanning electron microscope. Compared to scanning electron microscope (SEM), FESEM provides better resolution (up to 1 nm), which is essential when analyzing structures in the nanoscale. Primary electrons are liberated from the field emission source to bombard the sample. During the process, secondary electrons with characteristic angle and velocity at different spots are detected to produce electronic signals, which are eventually converted to produce a digital image of the sample. The field-emission source in FESEM provides narrower probing beam and higher electron energy which greatly improves the spatial resolution of FESEM, compared to SEM. The FESEM image of ZnO nanoparticles (Figure 3.1) shows the various sizes of the zinc oxide nanoparticles. From that figure, it can be roughly approximated via particle size distribution that the zinc oxide sizes are in the range of 20-50 nm.

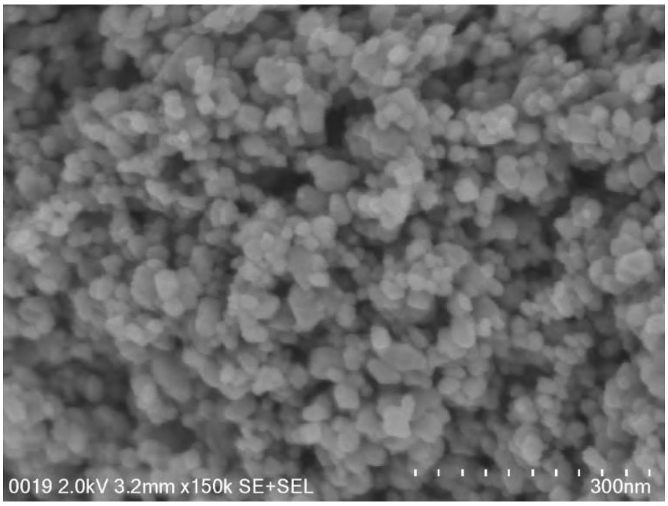

Figure 3.1: FESAM of the zinc oxide saturable absorber.

3.2.2 X-Ray Diffraction

X-ray diffraction (XRD) is a non-destructive technique to identify unknown materials, single crystal orientation, preferred orientation of crystals and many more, with minimal sample preparation. In XRD, the probing source is a collimated beam of x-rays with wavelengths in the range of 0.7-2.0 Å. The incident X-ray beam is diffracted by the crystalline phase of the sample. An XRD spectrum is a plot of the intensity of the diffracted beam plotted against the diffraction angle 2θ and the sample's orientation (Cao & Wang, 2004).

The XRD spectrum of the zinc oxide nanoparticles was also obtained and shown in Figure 3.2. The 100, 002, 101, 102, 110, 103 and 201 peaks confirm that the sample was indeed zinc oxide (Akhtar et al., 2012).

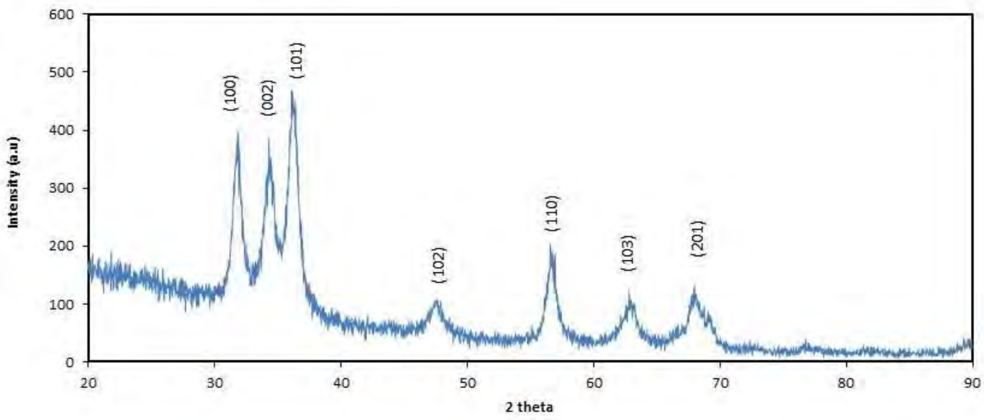

Figure 3.2: XRD of the ZnO saturable absorber.

3.3 Nonlinear Optical Characterization

The nonlinear absorption of ZnO SA was measured using the balanced twin-detector technique. The seed of the pulse was generated by passive mode-locking using graphene as a saturable absorber. The pulse has peak wavelength of 1560 nm with pulse width and pulse repetition rate of 0.81 ps and 27.7 MHz respectively. The mode-locked pulse was amplified using a low-dispersion amplifier before being attenuated using a variable optical attenuator. The output was divided equally using a 50/50 output coupler. One end of the coupler was connected directly to a power meter whereas the other end was connected to the ZnO SA before being measured by another identical power meter. The output power from the amplifier was attenuated gradually while the corresponding powers were registered simultaneously by the two identical power meters. The setup is depicted in Figure 3.3.

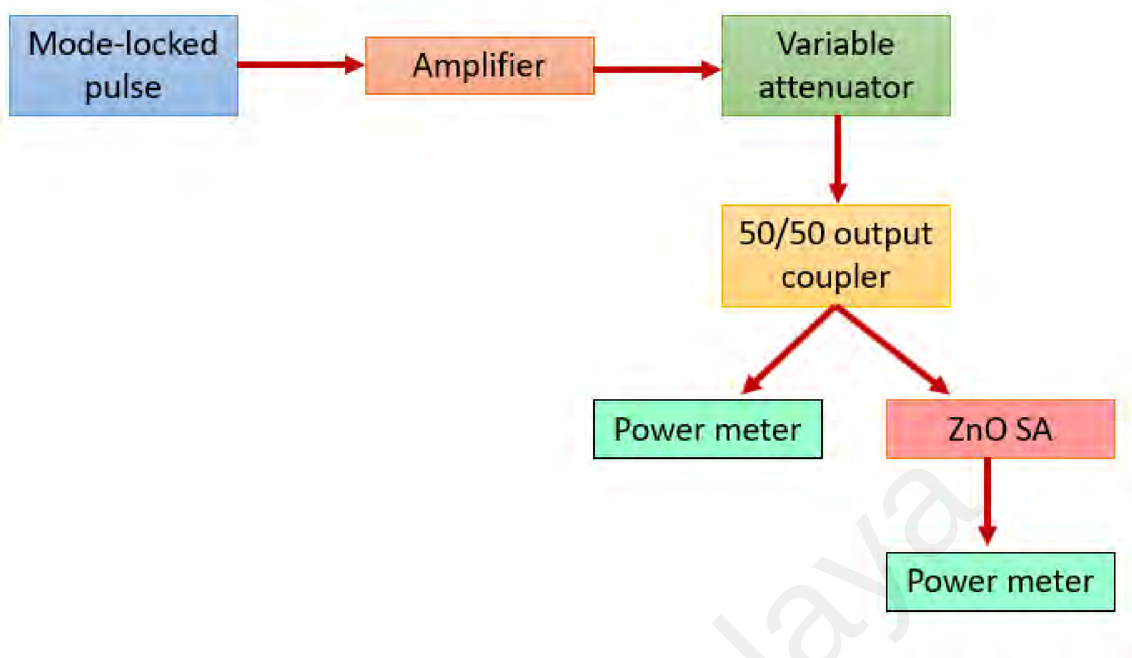

Figure 3.3: The setup of the balanced twin-detector system to measure the nonlinear absorption of the zinc oxide saturable absorber.

Using measurements from both the power meters, a plot of absorption against input intensities was plotted and fitted using equation 2.3. The fitted graph is shown in Figure 3.4 and the saturation intensity and modulation depth determined from the graph are 3.5 % and 0.016 $MWcm^{-2}$ respectively. This value of saturation intensity is very similar to the saturation intensity of titanium dioxide saturable absorber with a value of 0.013 MWcm^{-2} (H. Ahmad, Siti Aisyah Reduan, et al., 2016).

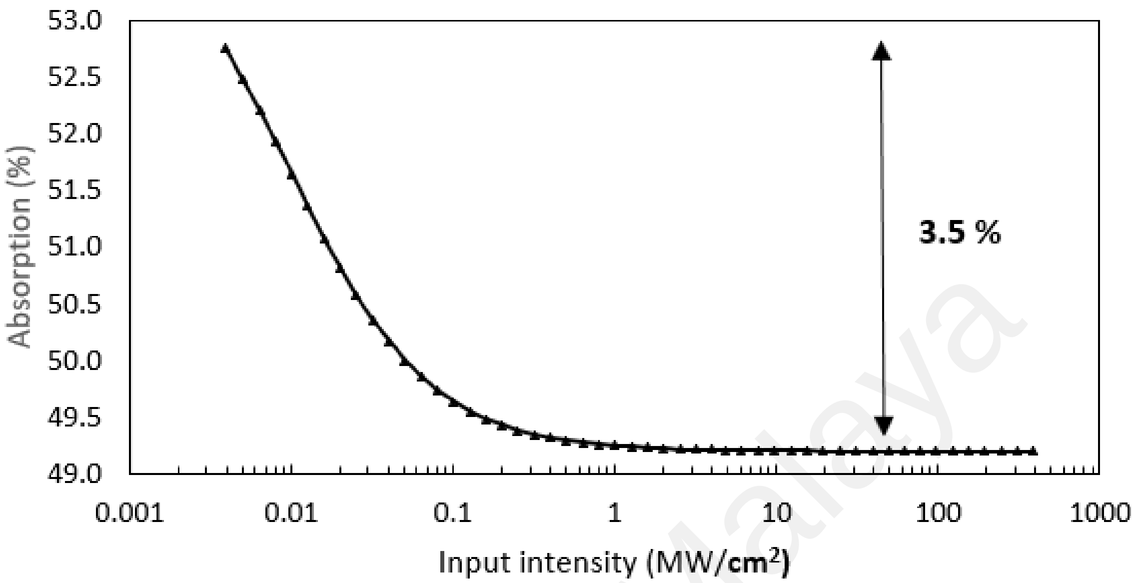

Figure 3.4: Nonlinear optical absorption of ZnO SA with modulation depth of 3.5%.

The ZnO SA was illuminated by white light source to determine the wavelength region of absorption and the insertion loss. The spectrum using ZnO SA was subtracted by the spectrum without the use of ZnO SA, to calculate the absorption of the ZnO SA. The resulted spectrum is illustrated in Figure 3.5 whereby the insertion loss and wavelength absorption region are determined. The ZnO SA has insertion loss of approximately 3.4 dB and exhibits broadband absorption of 1000-1600 nm, covering the S- band C-band regions as highlighted in Figure 3.5.

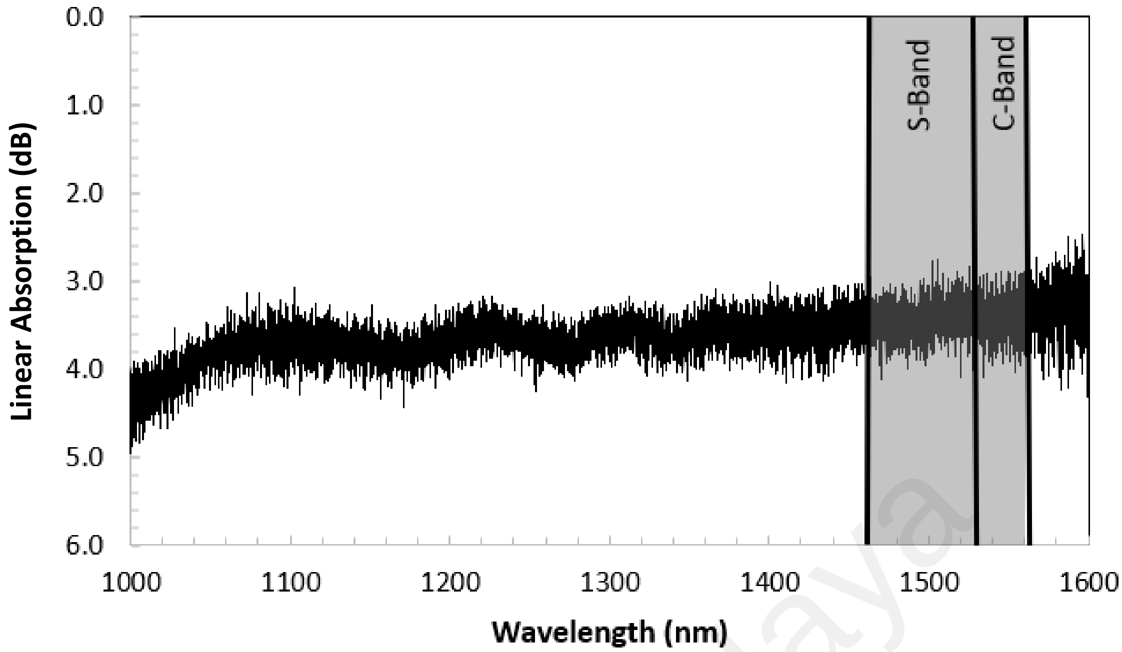

Figure 3.5: Absorption of ZnO SA when illuminated by a white light source.

CHAPTER 4: EXPERIMENTAL METHODS

After the fabrication and characterization of the zinc oxide saturable absorber, the saturable absorber was incorporated into several laser cavity setups. In this Chapter, the cavity setups to obtain Q-Switching in C-band and S-band using zinc oxide saturable absorber are described.

4.1 Passive Q-Switching in C-Band

The ZnO SA was integrated into the cavity by sandwiching two layers of ZnO thin films between two fiber ferrules. The ZnO films was held in position using index matching gel.

The laser's source pump was a 974 nm laser diode and the gain medium used was a 3-m long erbium-doped fiber (EDF). The EDF used was Fibercore M-12(980/125) with 911 nm cut-off wavelength, has mode field diameter of 6.6 μm and exhibits peak absorption at 18.06 dB/m. The laser diode was coupled to the EDF via a wavelength division multiplexer (WDM). A 90/10 output coupler was used which allow 90% of the light to resonate inside the cavity while the remaining 10% was channelled to another 50/50 coupler for simultaneous measurements of the light signal. To make sure that the light was propagating in a single direction in the cavity, an optical isolator was placed between the 90/10 output coupler and WDM. The setup of the cavity is illustrated in Figure 4.1. The overall cavity had an approximate length of 19 m.

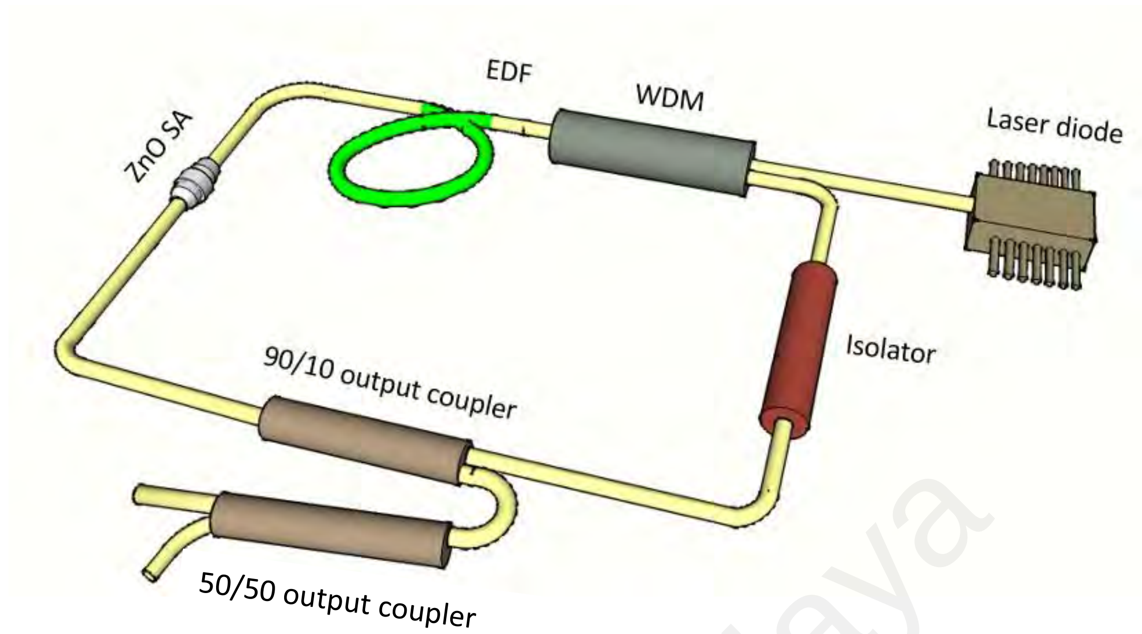

Figure 4.1: The setup of the cavity for Q-switching in C-band.

ZnO exhibits birefringence in the order of several terahertz (Kim, Ahn, Kim, & Yee, 2011), hence none of the components used were polarization-sensitive. Furthermore, the use of polarization controller was avoided to eliminate the possibility of Q-switching due to nonlinear polarization rotation technique. No Q-switching was observed when the ZnO SA was removed, confirming that the Q-switching was initiated by the saturable absorber and not by any other components used in the cavity.

For measurements of the characteristics of the Q-switching pulse, several instruments were connected to the 50/50 output coupler. The output power was measured by an optical power meter, the pulse repetition rate was measured by a 500 MHz oscilloscope made by Yokogawa connected via a 1.2 GHz photodetector. The wavelength spectrum was obtained using an optical spectrum analyser (Yokogawa) whereas the radio-frequency spectrum was obtained using a radio-frequency spectrum analyser (Anritsu).

4.2 Tunable Q-Switching in C-Band

To determine the tuning range of the Q-switching, a tunable bandpass filter was placed between the gain medium and the saturable absorber, as illustrated in Figure 4.2. The tunable filter had a tuning range of 40 nm with insertion loss of 3 dBm and central wavelength of 1550 nm. The total length of this cavity was 20 m.

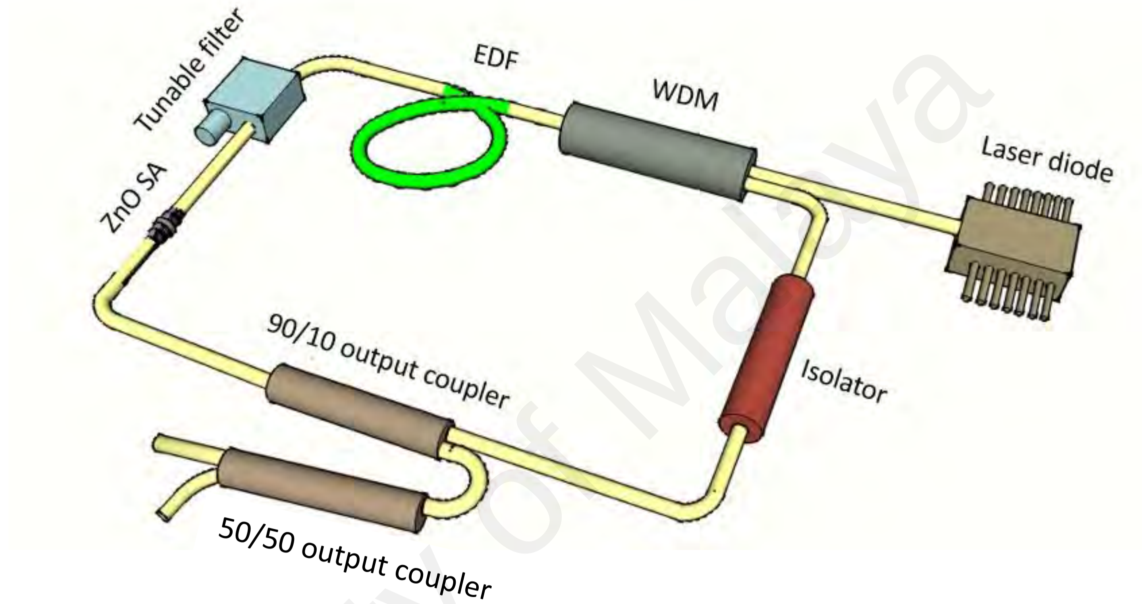

Figure 4.2: The cavity setup for tunable Q-switched laser in C-band.

The output power, spectra and time profile of the Q-switched pulse were obtained using the same instruments as described previously. These measurements were recorded at every 2 nm intervals as the tunable bandpass filter tuned the wavelength of the laser from 1536 nm to 1586 nm.

4.3 Passive Q-Switching in S-Band

The main difference between passive Q-switching in S-band and C-band is the type of gain medium used. In C-band, the gain medium was a standard EDF whereas in S-band, the type of gain medium was a special type of EDF known as depressed-cladding erbium-doped fiber (DC-EDF).

Figure 4.3 shows the cavity configuration to obtain Q-switched laser in S-band using ZnO saturable absorber. A 15-m DC-EDF was used as the gain medium instead of a standard EDF. A standard EDF exhibits strong amplified spontaneous emission (ASE) in C-and L-band while ASE at shorter wavelengths is suppressed. Unlike EDF, DC-EDF has a refractive index profile that enables the distributed loss to be lower than the erbium gain in S-band regime. Beyond this regime, the distributed loss is much higher than the erbium gain. As such, the fundamental mode cut-off wavelength of DC-EDF is near 1525 nm (Arbore et al., 2002), allowing ASE to be observed in S-band. Due to DC-EDF sensitivity to bending, the fiber spool was maintained at 7 cm, within the optimum spooling diameter as reported in (H. Ahmad, Saat, & Harun, 2005).

Two thin films of ZnO nanoparticles were pasted on the surface of two fiber ferrules, connected via a fiber connector to form a fiber compatible SA (ZnO SA). The DC-EDF was connected to a polarisation-independent isolator to ensure unidirectional light propagation in the ring cavity. A 95/5 optical output coupler was used to tap 5% of the light signal for monitoring purposes while the 95% port was connected to the ZnO SA. The signal was monitored simultaneously by an optical power meter and oscilloscope via a 50/50 optical output coupler. To complete the laser cavity ring, a wavelength division multiplexing (WDM) device was coupled into the cavity with the common port (1520 nm) connected to the DC-EDF, while the 980 nm port and 1550 nm port were connected to a 974 nm laser diode and the ZnO SA respectively. The cavity had a total length of 33 m.

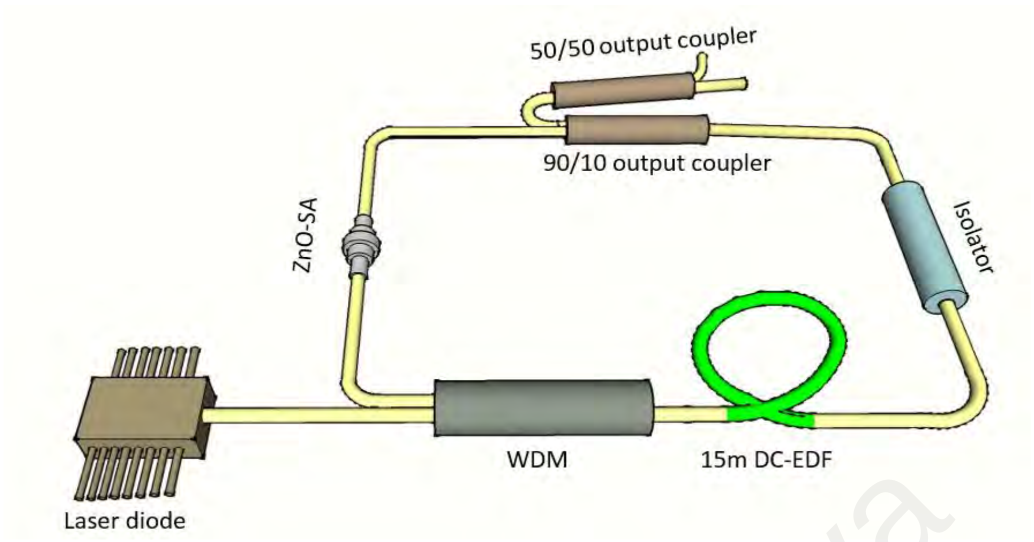

Figure 4.3: The cavity setup for passive Q-switching in S-band.

4.4 Tunable Q-switching in S-band

The setup for tunable Q-switching was almost similar to the cavity for passive Q-switching for S-band with an additional of a tunable bandpass placed between the isolator and the 90/10 output coupler, as shown in Figure 4.4. As the tunable bandpass filter tuned the wavelength of the laser, the output power, spectra and time profile of the pulse were recorded at every 2 nm intervals.

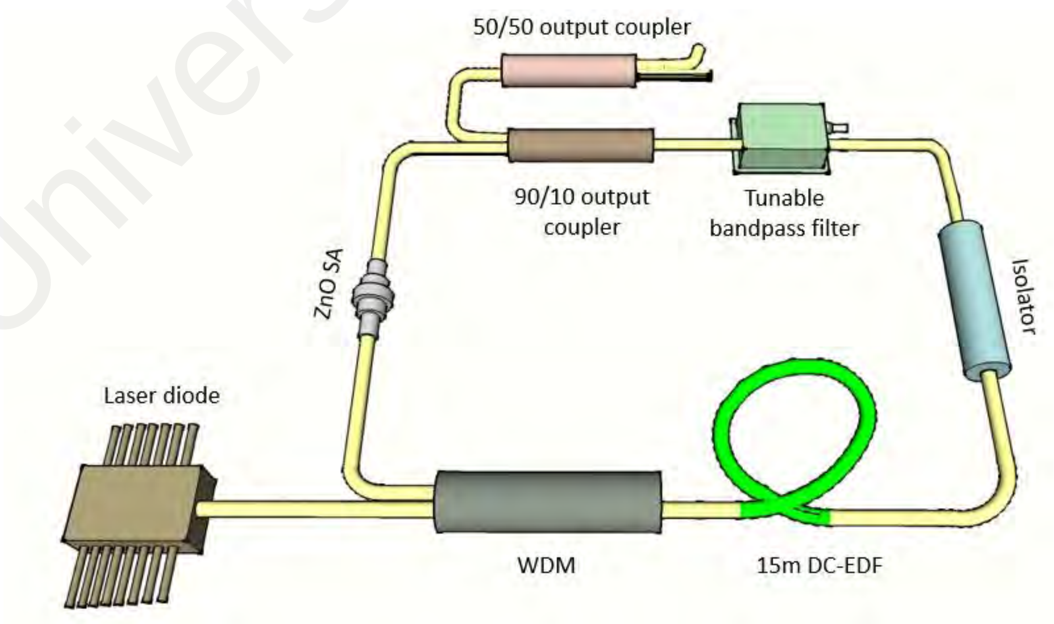

Figure 4.4: The cavity setup for tunable Q-switching in S-band.

CHAPTER 5: EXPERIMENTAL RESULTS AND DISCUSSIONS

The main results from all the experiments described in the previous chapter will be presented in this chapter.

5.1 Passive Q-Switching in C-Band

Continuous wave was observed when the laser was pumped at 20 mW. At 60 mW, self-started Q-switching was observed. The optical spectrum and time profile of the pulse at this pump power is shown in Figure 5.1(a) and (b). The laser has a peak wavelength at 1561 nm.

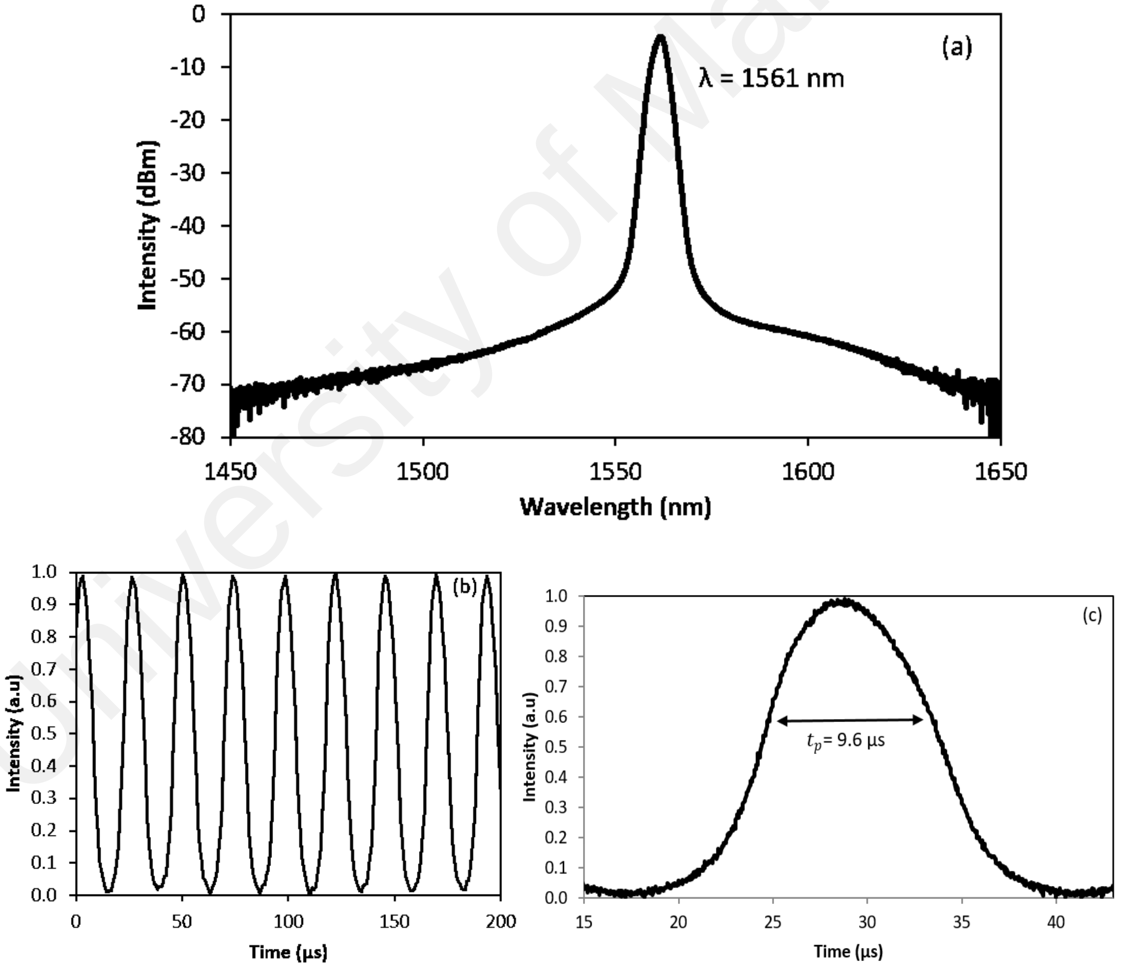

Figure 5.1: (a) The optical spectrum, (b) time profile and (c) pulse width of the Q-switched pulse at 60 mW.

As the power increased gradually from 60 mW to 360 mW (the maximum pump power available), the repetition rate increased from 42 kHz to 77 kHz whereas the pulse width decreased from 9.6 µs (Figure 5.1 (c)) to 3.0 µs, as shown in Figure 5.2. This trend of increasing repetition rate and decreasing pulse width as the pump power increases is very typical of Q-switched pulse (Svelto, 2010) whereas this trend is not observed in mode-locked pulse which has a fundamental repetition rate.

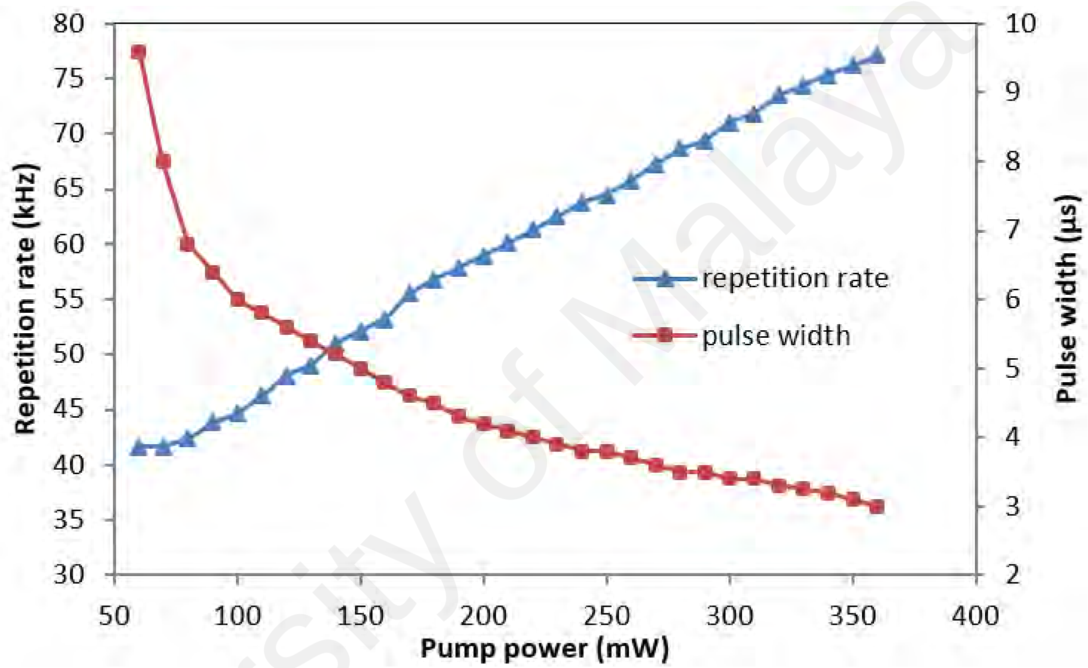

Figure 5.2: The trend of repetition rate and pulse width with increasing pump power.

As the pump power increased, the corresponding pulse energy and peak power were calculated using equations 2.1 and 2.2 respectively. The variation of pulse energy and peak power with pump power is shown in Figure 5.3 whereby the trendline of the pulse energy is very similar to the trend of output power against pump power (Figure 5.4). The maximum pulse energy is 48 nJ which is higher than the maximum pulse energy using graphene (Popa et al., 2011), MoS_2 (Li et al., 2015) and TiO_2 (H. Ahmad, Siti Aisyah Reduan, et al., 2016) saturable absorbers. The maximum pulse energy can be further increased by using a larger mode area fiber and changing the output coupler which allows more energy to be tapped out. From Figure 5.3, the variations of both the pulse energy and peak power show a steady increase and then a slight decrease. Although repeated measurements had been made, similar trend was observed. A possible explanation for this observation is the saturable absorber might have reached its damage threshold whilst the pump power was gradually increased.

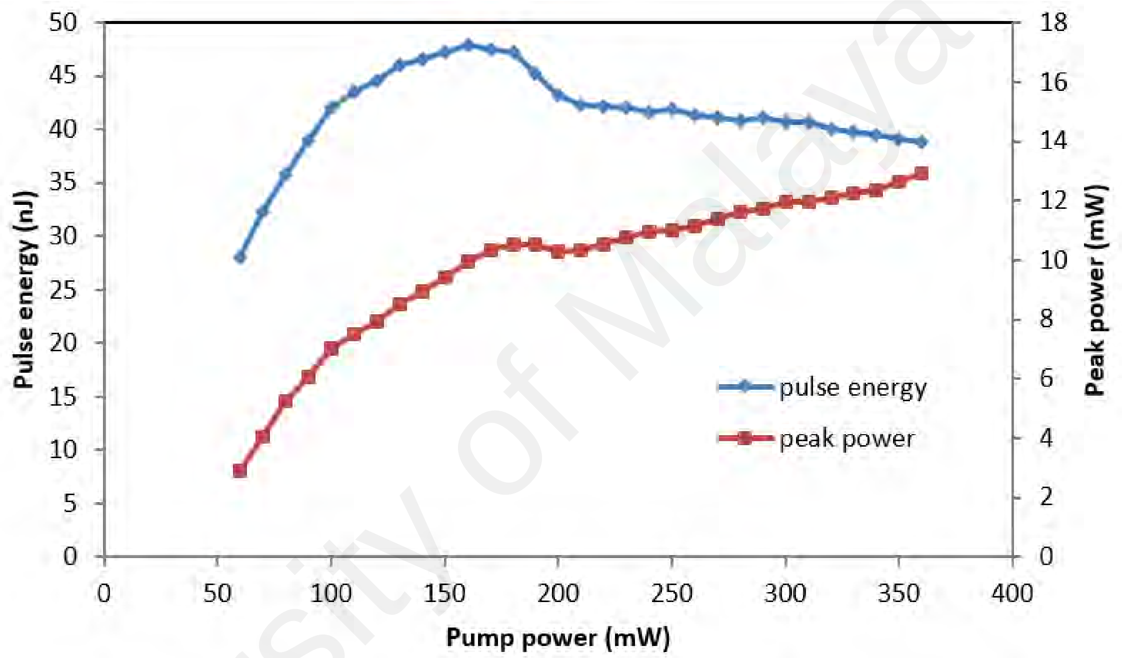

Figure 5.3: The variation of pulse energy and peak power with increasing pump power.

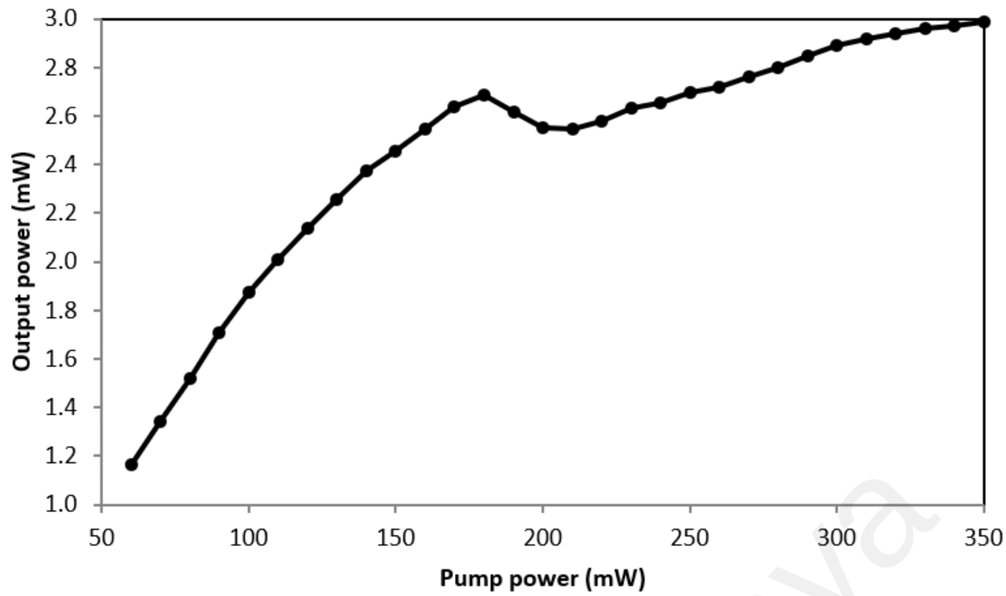

Figure 5.4: The graph of output power against pump power.

The radio-frequency spectrum obtained at 41.7 kHz (Figure 5.5) shows that it has a high signal-to-noise ratio (SNR) of 56 dB, which is higher than the SNR using graphene saturable absorber (~40 dB) (Popa et al., 2011).

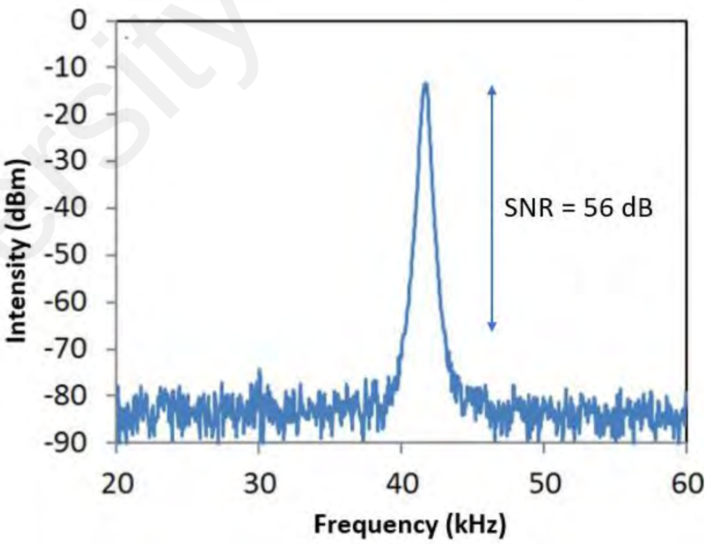

Figure 5.5: The radio-frequency spectrum of the pulse at repetition rate of 41.7 kHz with SNR of 56 dB.

5.2 Tunable Q-Switching in C-Band

With the addition of a tunable bandpass filter as a part of the cavity, the laser performance will be characterized in two ways. Firstly, the pump power was varied while the wavelength was fixed at a value of 1561 nm. Secondly, the wavelength was varied using the tunable bandpass filter while the pump power was maintained at a value of 190 mW.

At a fixed wavelength of 1561 nm, Q-switching was observed starting at 80 mW up until the maximum available pump power of 360 mW. As the pump power increased, the repetition rate increased from 39 kHz to 70 kHz, while the pulse width decreased from 2.4 μs to 1.7 μs, as shown in Figure 5.6. Above pump power of 180 mW, the pulse width reached a plateau which might be attributed to the saturation of the upper energy level of the EDF (Chen et al., 2014). The variations of the output power, pulse energy and peak power as the pump power increases are shown in Figure 5.7 and Figure 5.8. The maximum pulse energy is 40 nJ. The pulse has a good SNR of 42 dB, obtained from its radio-frequency spectrum (Figure 5.9).

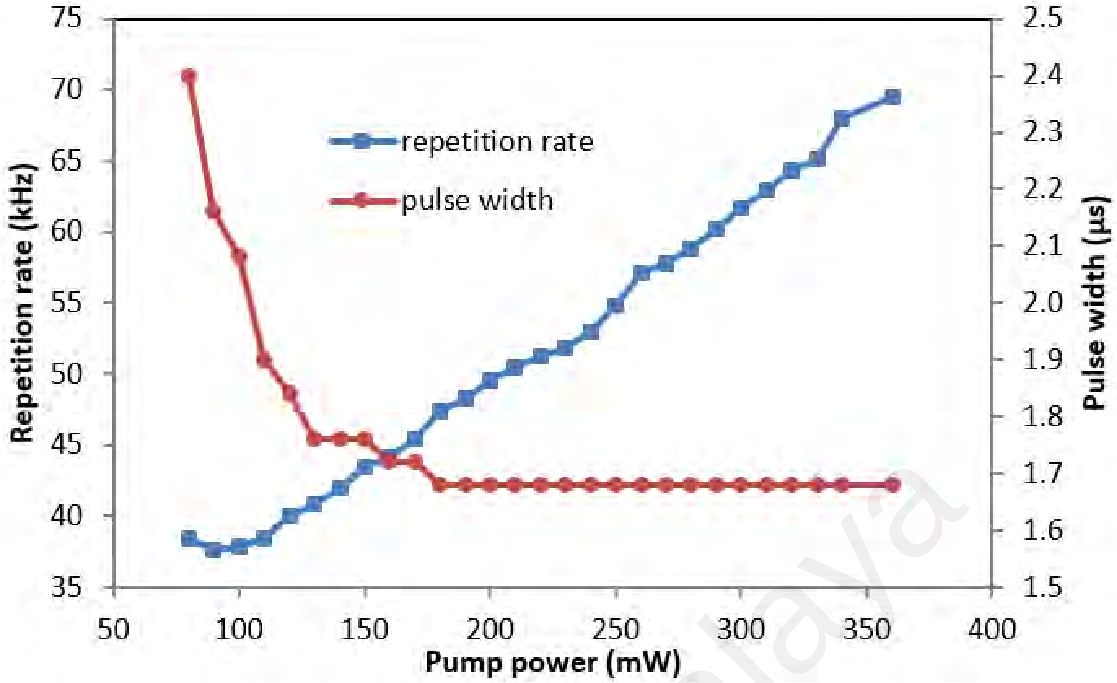

Figure 5.6: Variations of repetition rate and pulse width as the pump power increases.

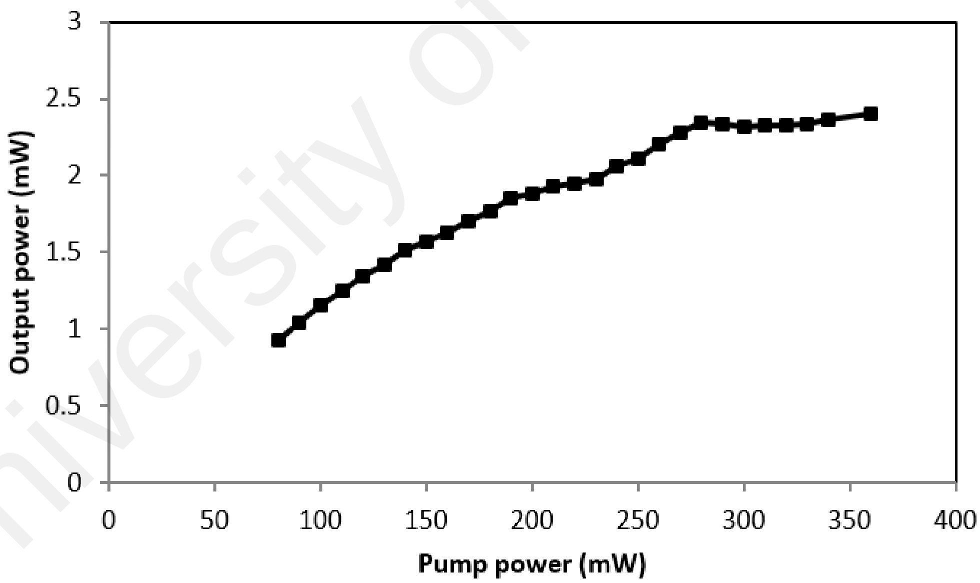

Figure 5.7: Output power against pump power.

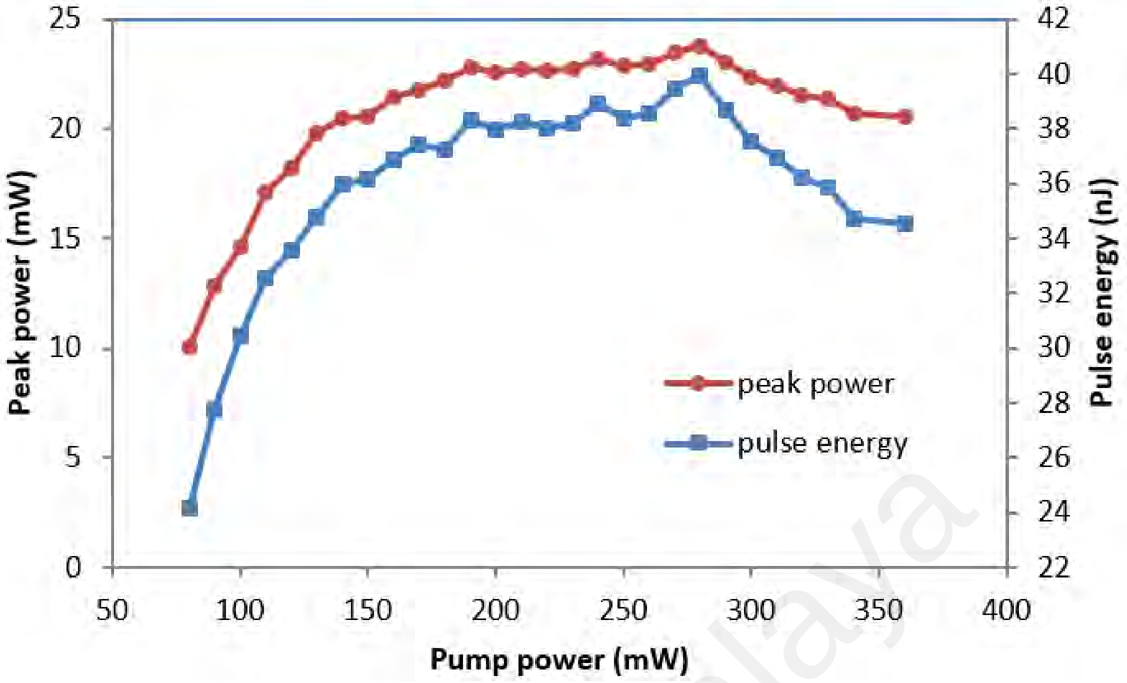

Figure 5.8: Variations of peak power and pulse energy as pump power increases.

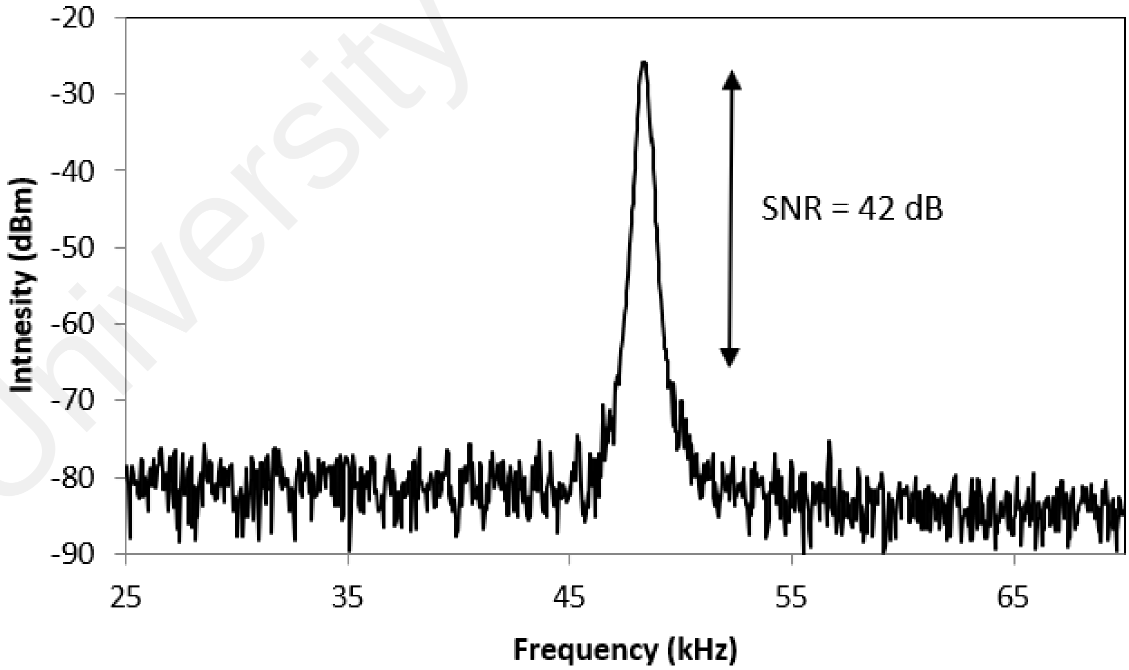

Figure 5.9: The radio-frequency spectrum of the pulse with SNR of 42 dB.

The tunability of the ZnO SA was investigated by varying the wavelength of the laser while fixing the pump power at 190 mW. Q-switching was observed as the wavelength was varied from 1536 nm to 1586 (Figure 5.10), covering a range of 50 nm which was wider the tuning range achieved using MoS_2 (48.1 nm) (Huang et al., 2014) and graphene (32 nm) (Popa et al., 2011) saturable absorbers. The tuning range was limited by the tunable bandpass filter and not by the saturable absorber. Hence, the tuning range could be further enhanced by using a bandpass filter with a tuning range larger than 50 nm.

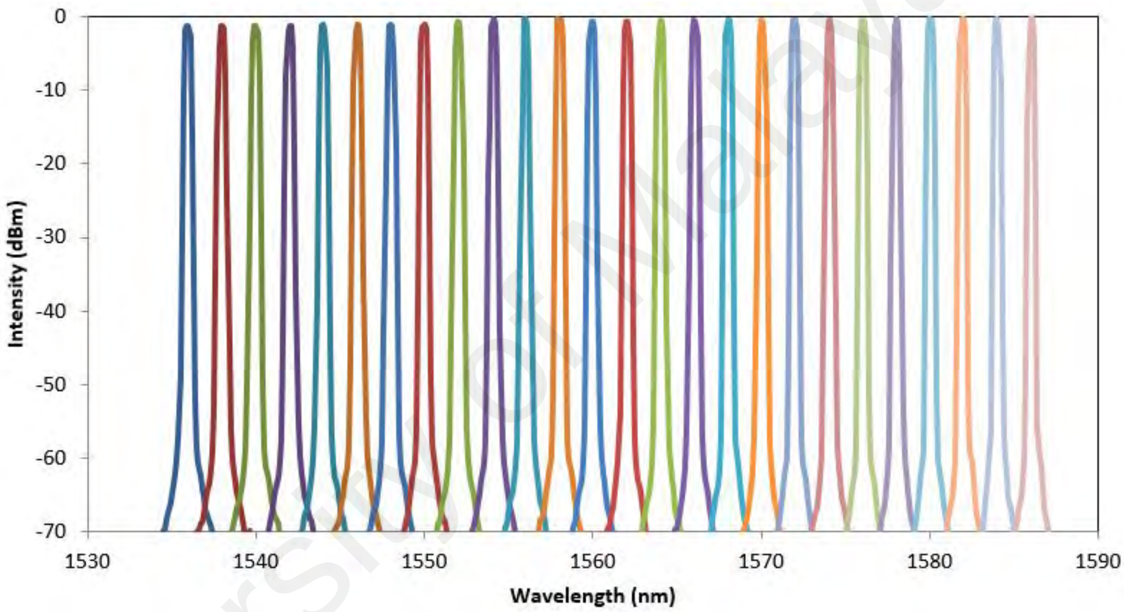

Figure 5.10: Optical spectra of the Q-switched laser as the wavelength was varied from 1536 nm to 1586 nm.

As the wavelength increased, the pulse width expanded from 2.9 μs to 4.5 μs whereas the repetition rate reduced from 64 kHz to 29 kHz (Figure 5.11). The trend of the repetition rate follows closely to the trend of the amplified spontaneous emission at the same wavelength range, as highlighted in the inset of Figure 5.11. At a particular high-gain wavelength, the intracavity lasing is stronger, which allow bleaching of the ZnO saturable absorber to occur much faster and hence increases the repetition rate. This explains the similarities between the trend of repetition rate and the trend of the amplified spontaneous emission.

The peak power and pulse energy increased as the wavelength increased, as illustrated in Figure 5.12, with a maximum pulse energy of 46 nJ. However, the output power did not vary much (Figure 5.13). With an average output power of 1.2 mW and standard deviation of 0.08 mW, suggesting that the output power was not strongly dependent on small change in lasing wavelength.

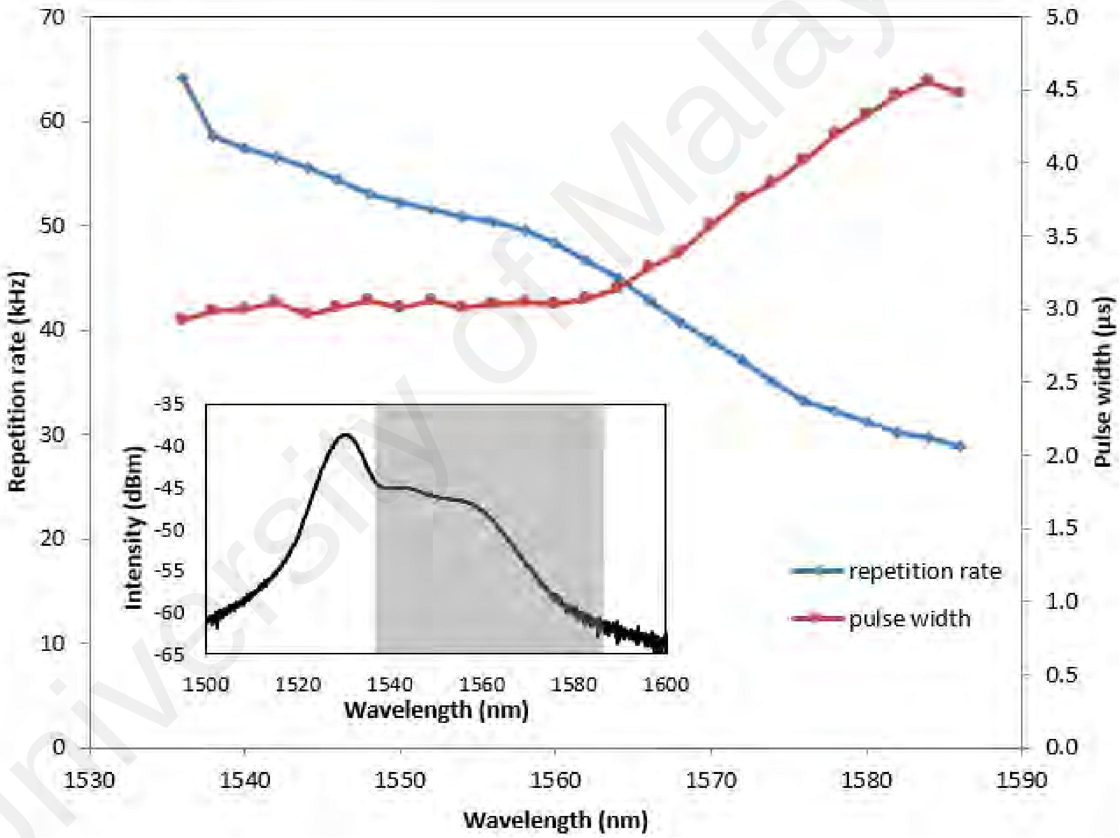

Figure 5.11: Plot of repetition rate and pulse width against different wavelengths. The inset shows the amplified spontaneous emission of the laser with the range covered by the Q-switching highlighted.

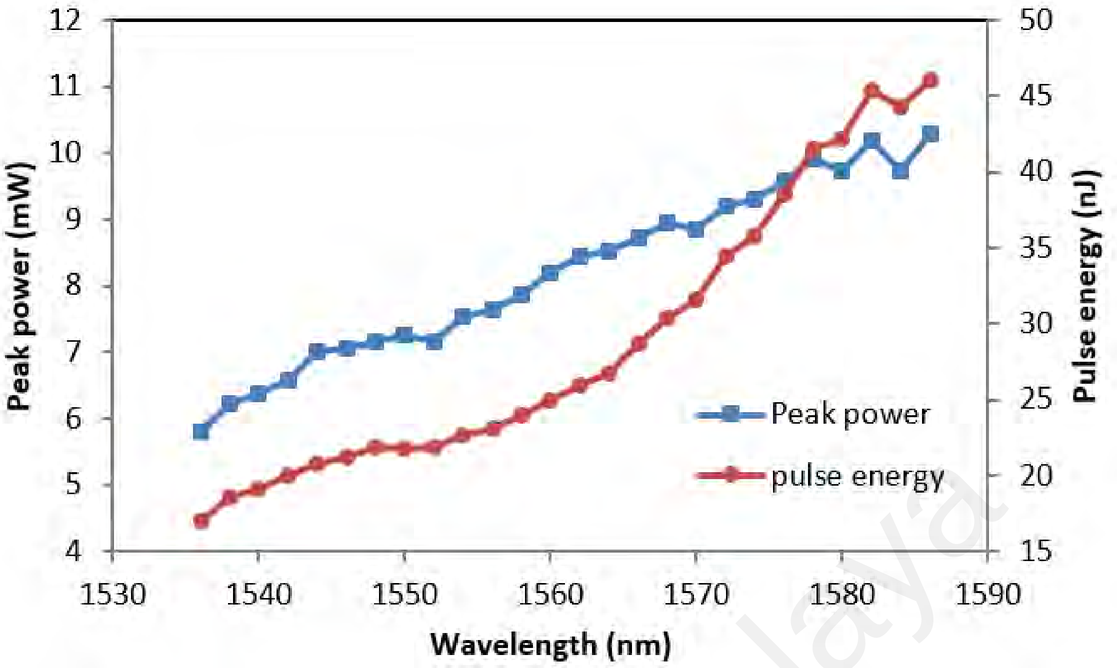

Figure 5.12: Plot of peak power and pulse energy against wavelength.

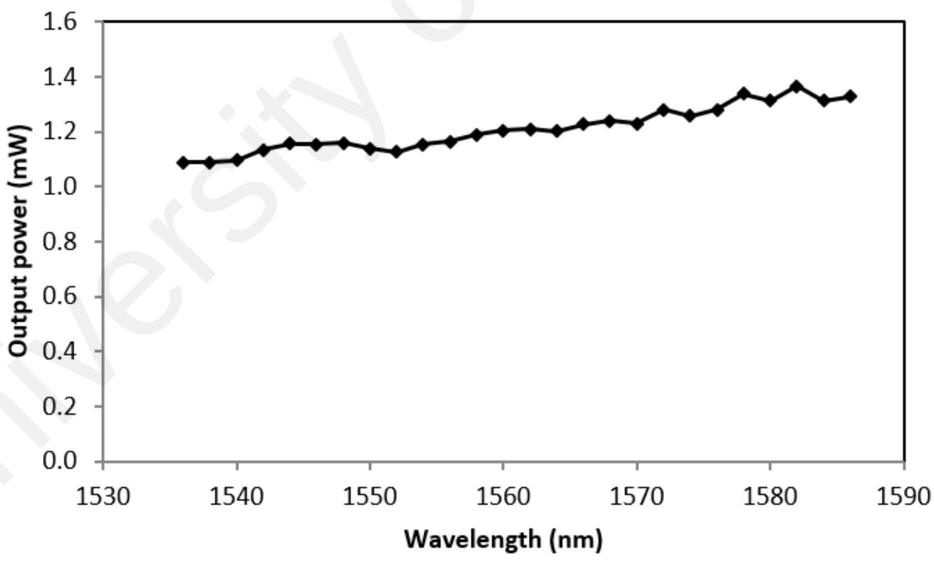

Figure 5.13: Output power as a function of lasing wavelength.

The results of ZnO saturable absorber was compared to other saturable absorbers as shown in Table 5.1.

Saturable absorbers	**ZnO**	**TiO_2**	**MoS_2**	**$MoSe_2$**	**Graphene**
Modulation depth (%)	3.5	35.41	2	4.7	-
Saturation intensity (MW/cm^2)	0.016	0.013	10	3.4	-
Repetition rate (kHz)	29 - 64	80 - 120	10.6 - 34.5	26.5- 35.4	36-103
Pulse width (µs)	2.9 - 4.5	1.8 -2.1	5 -9	18.9-9.2	~ 2
Maximum pulse energy (nJ)	46	2.2	160	825	~ 40
Tuning range (nm)	50	-	48.1	-	32
References		(H. Ahmad, Siti Aisyah Reduan, et al., 2016)	(Huang et al., 2014)	(R. I. Woodward, Howe, Runcorn, et al., 2015)	(Popa et al., 2011)

Table 5.1: The comparison of zinc oxide saturable absorber to other saturable absorbers.

Zinc oxide has the largest tuning range among these saturable absorbers. It also has a much larger maximum pulse energy than TiO_2. However, TiO_2 may be useful in applications where smaller pulse energy with high repetition rate is required. Among all these saturable absorbers, zinc oxide has the most similarities (pulse width, maximum pulse energy, tuning range) to graphene.

5.3 Passive Q-Switching in S-Band

Continuous wave operation started at pump power of 30 mW. Stable Q-switched pulse with a peak at wavelength of 1500 nm (Figure 5.14) was initiated at pump power of 170 mW, higher than the initial pump power (60 mW) needed for Q-switching in C-band using the same SA as reported in Section 5.1. Q-switched pulse was continuously observed as the pump power was consistently increased from 170 mW to 380 mW, the maximum available pump power. Figure 5.15 shows the corresponding radio-frequency spectrum with a good signal-to-noise ratio (SNR) of approximately 32 dB, verifying that the Q-switched pulse observed was stable. The pulse trains at different pump powers are illustrated in Figure 5.16 (a) and (b), obtained using an oscilloscope. The pulse trains at these pump powers did not show any obvious jitterings, further confirming that the pulses were stable.

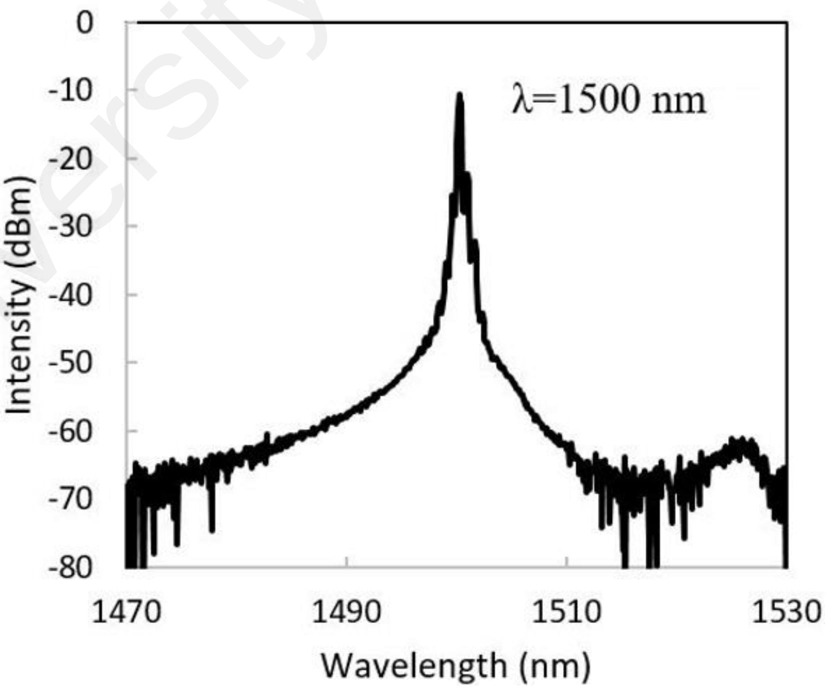

Figure 5.14: Optical spectrum with a peak at 1500 nm at pump power of 170 mW.

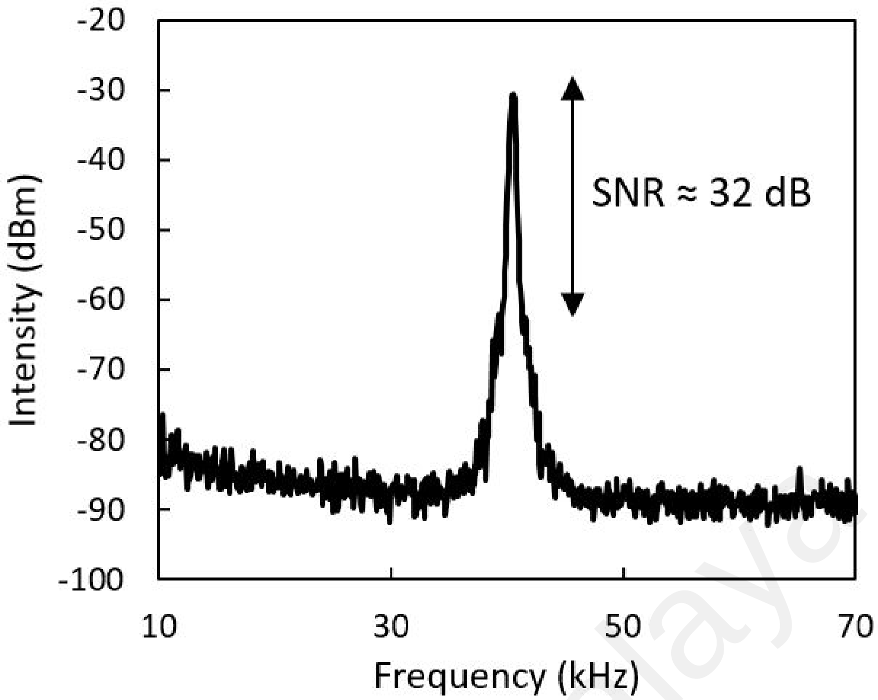

Figure 5.15: The radio-frequency spectrum with resolution bandwidth of 0.3 kHz at fundamental frequency of 41.9 kHz with SNR approximately 32 dB.

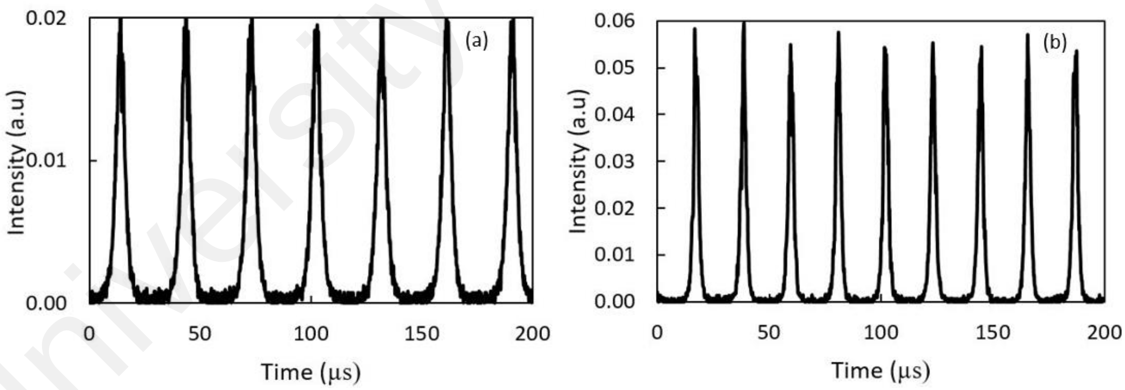

Figure 5.16: Pulse trains at pump power of (a) 200 mW and (b) 360 mW.

As the pump power was gradually increased, the repetition rate increased from 30.3 kHz to 48.1 kHz whereas the pulse width decreased from 5.4 μs to 2.3 μs (Figure 5.17). The pulse widths were significantly shorter than the pulse widths obtained using bismuth selenide as saturable absorber operating in S-band (H. Ahmad et al., 2015).

However, even shorter pulse width could theoretically be achieved by reducing the cavity length (Degnan, 1995). The pulse energy and peak power at various pump power were calculated and presented in Figure 5.18. The pulse energy increased linearly from 1.7 nJ to 3.2 nJ while the peak power rose from 0.3 mW to 1.4 mW as the pump power was raised. Although the maximum pulse energy using ZnO SA was much lower than other conventional saturable absorber such as graphene (~ 40 nJ) (Popa et al., 2011) and MoS_2 (~ 100 nJ) (R. I. Woodward et al., 2014), the pulse energy was slightly higher than the maximum pulse energy obtained using titanium dioxide (~ 2.2 nJ) (H. Ahmad, Siti Aisyah Reduan, et al., 2016), which is suitable for applications that require high repetition rate and low pulse energy.

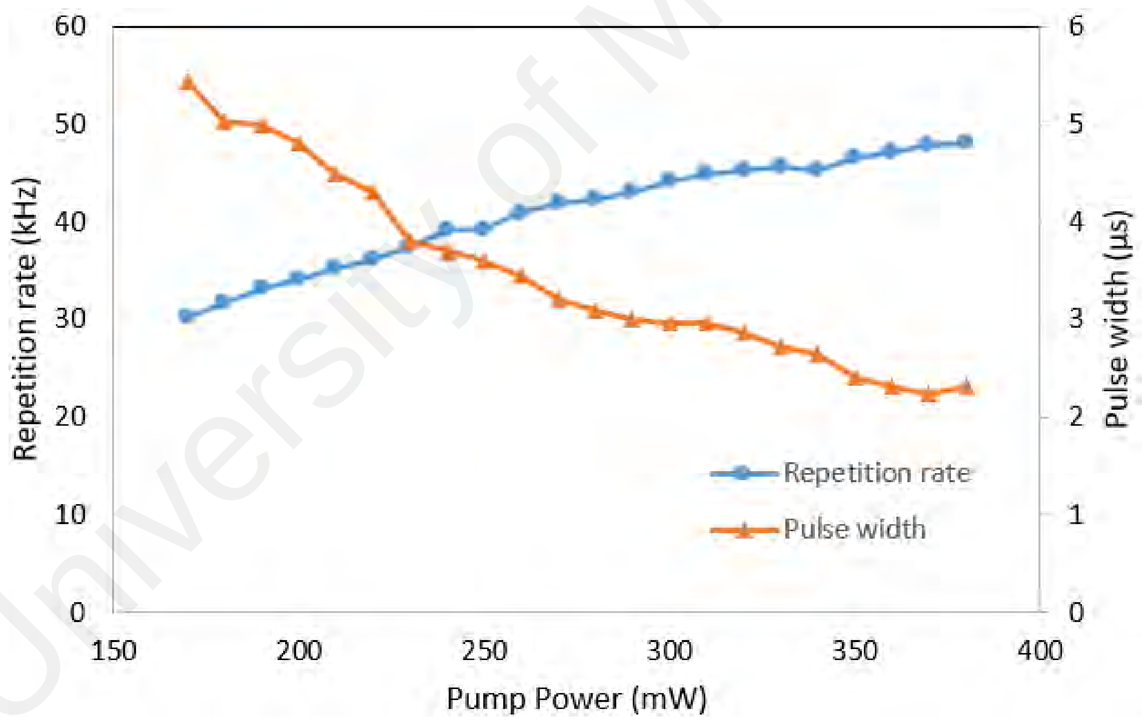

Figure 5.17: Variation of repetition rate and pulse width with pump power.

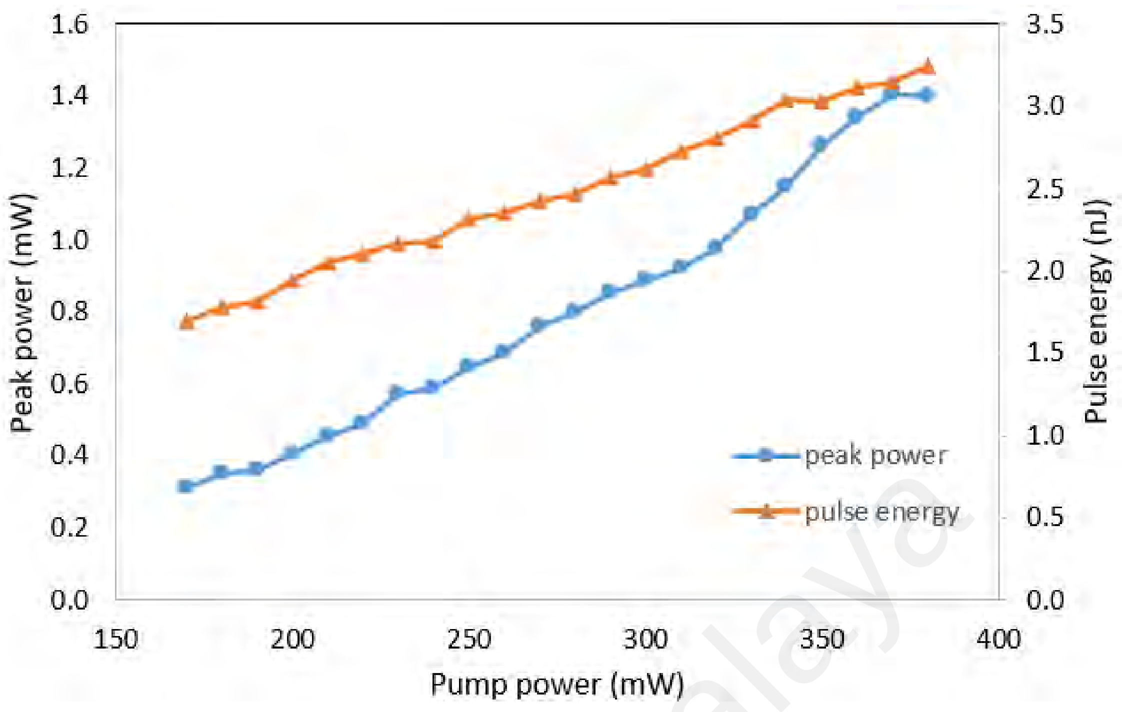

Figure 5.18: Variation of peak power and pulse energy with pump power.

5.4 Tunable Q-Switching in S-Band

When the tunable bandpass filter was inserted into the S-band cavity, the repetition rate increased from 28 kHz to 37 kHz while the pulse width reduced from 2.8 μs to 1.0 μs as the pump power was increased from 250 mW to 380 mW while maintaining the lasing wavelength at 1490 nm, as shown in Figure 5.19. The variation of peak power and pulse energy with increasing pump power is displayed in Figure 5.20. However, it has a low SNR of approximately 27 dB, estimated from its radio-frequency spectrum as shown in Figure 5.21.

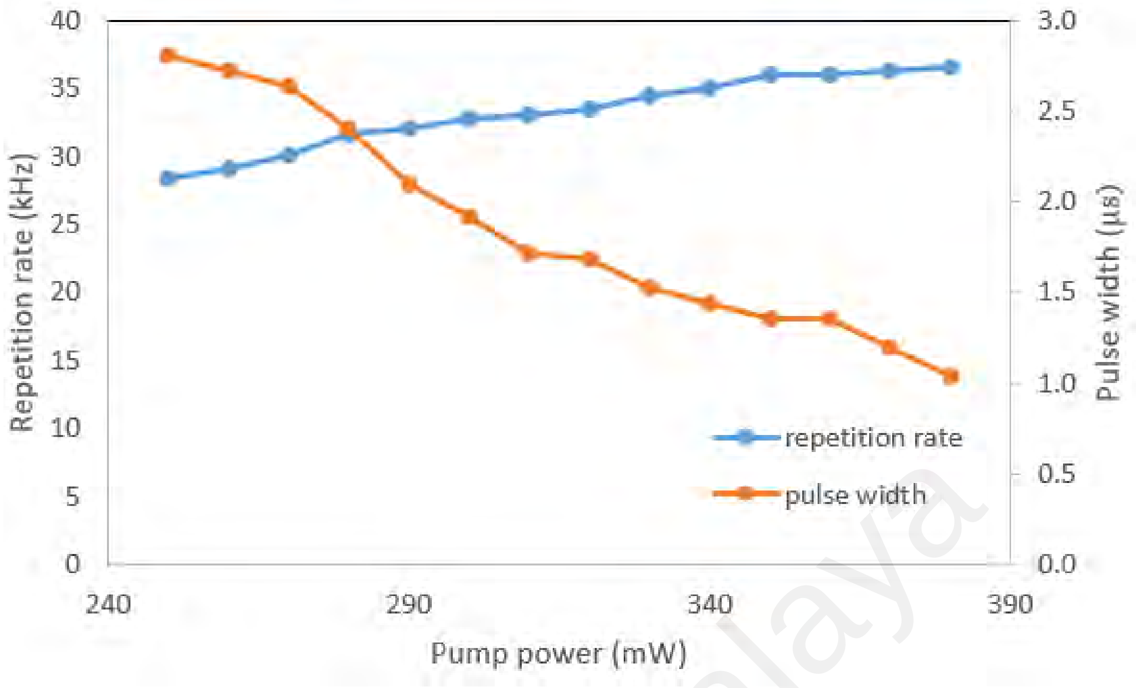

Figure 5.19: The variation of repetition rate and pulse width with increasing pump power at lasing wavelength of 1490 nm.

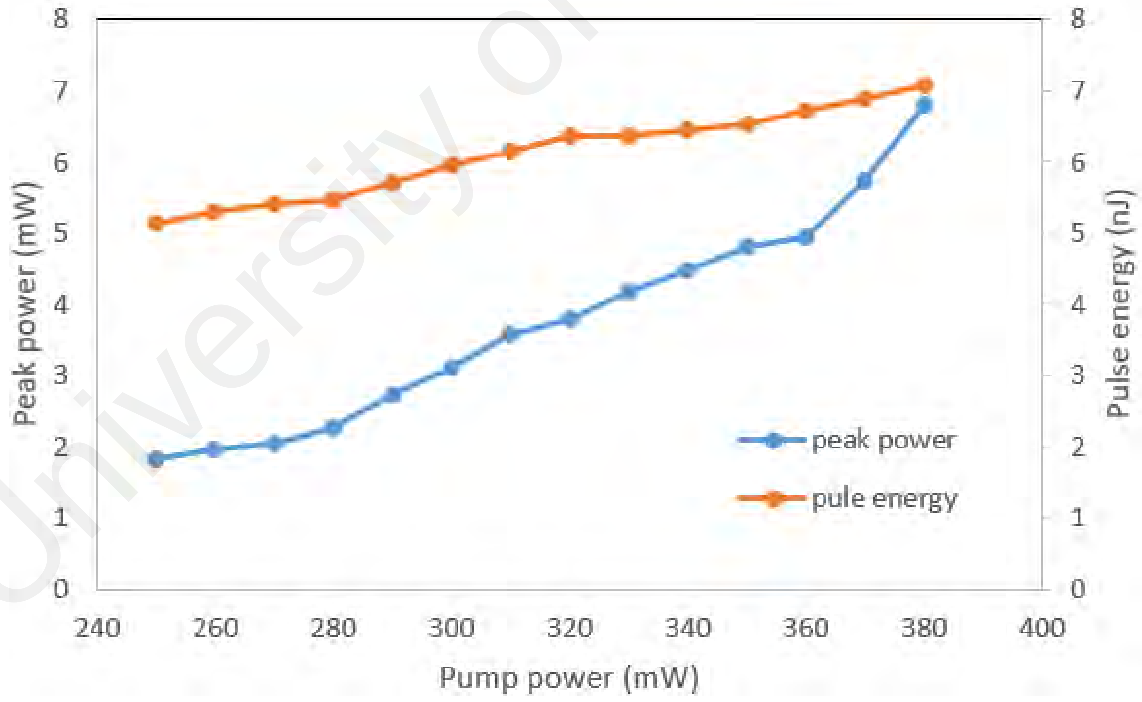

Figure 5.20: The variation of peak power and pulse energy with increasing pump power at lasing wavelength of 1490 nm.

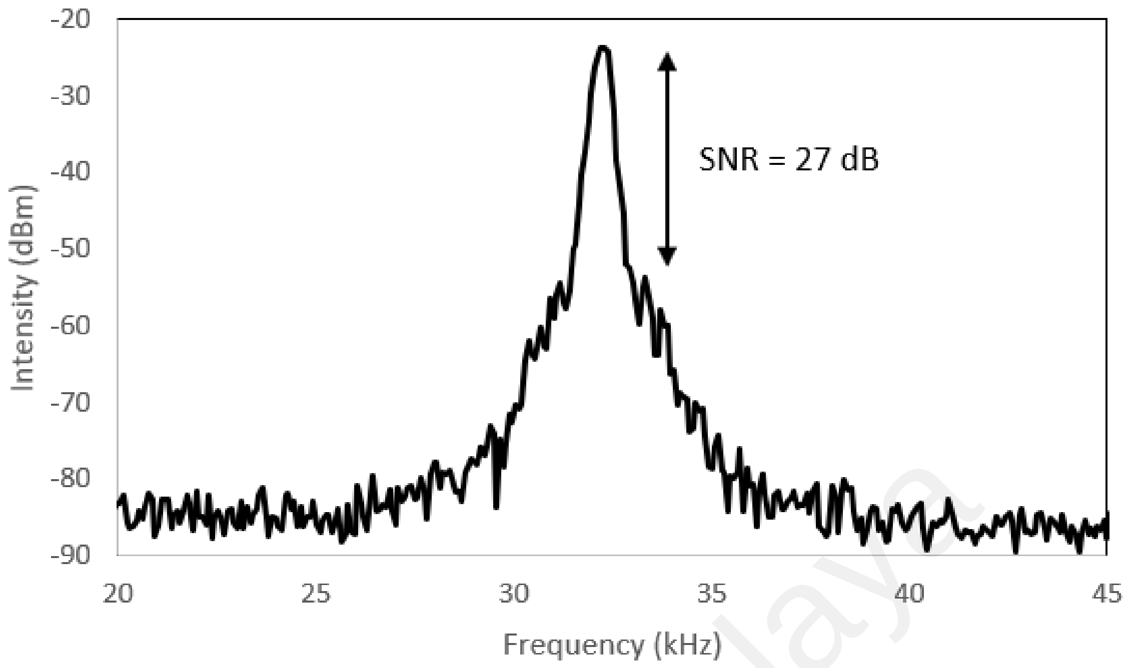

Figure 5.21: The radio-frequency spectrum of the S-band laser at frequency of 32 kHz.

To investigate the tunability of the laser using the ZnO saturable absorber, the lasing wavelength was varied from 1484 nm to 1500 nm, using a tunable bandpass filter while the pump power was maintained at a constant value of 310 mW. Their optical spectra are presented in Figure 5.22, with their peaks not as sharply defined as the peaks observed in the case of C-band (Figure 5.10).As the wavelength was gradually increased at interval of 2 nm, the pulse width decreased from 2.8 μs to 1.1 μs whereas the repetition rate increased from 29 kHz to 39 kHz. Although the trends of repetition rate and pulse width follow the typical characteristics of Q-switched pulse as shown in Figure 5.19, its poor SNR value and uneven peak observed in their optical spectra, imply that the quality of the Q-switched pulse is low. The tunable filter with central wavelength of 1550 nm may not be suitable for application and distort the quality of the Q-switched pulse. A straightforward solution for future work is to replace the tunable bandpass filter with another tunable bandpass filter with central wavelength in the S-band region.

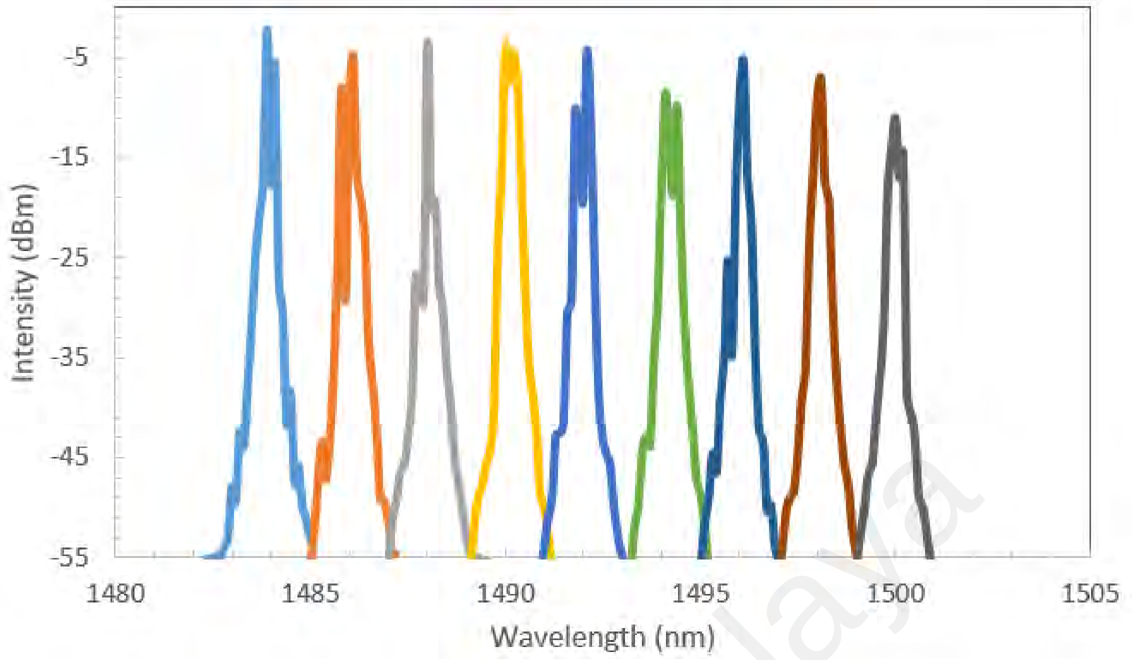

Figure 5.22: The optical spectra at various wavelengths in the S-band region.

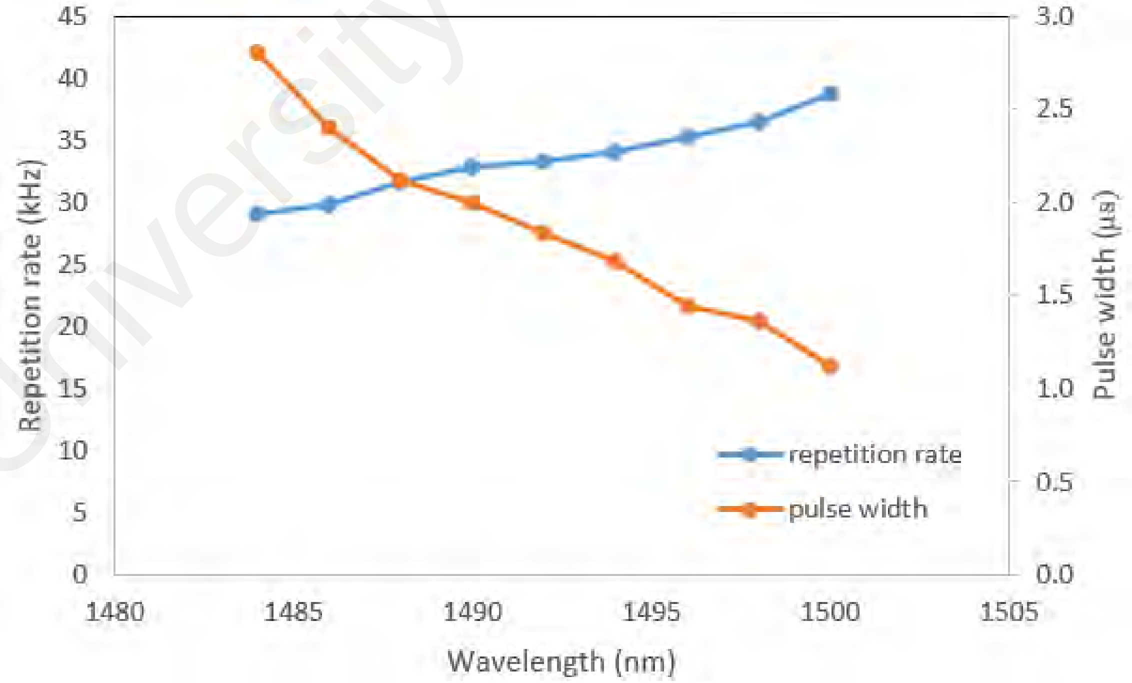

Figure 5.23: The variation of repetition rate and pulse width as the wavelength increased from 1484 nm to 1500 nm.

CHAPTER 6: CONCLUSION

The major focus of this work is to explore the possibility of using zinc oxide as a saturable absorber in passive Q-switching. Its picosecond recovery time and high optical nonlinearity made ZnO a suitable choice as a saturable absorber for passive Q-switching.

The ZnO nanoparticles obtained, was in powder form. In order to integrate the nanoparticles into the laser cavity, thin films of ZnO nanoparticles were developed. The thin films were then placed in between two fiber ferrules using index matching gel to form a fiber compatible saturable absorber. The ZnO nanoparticles were then characterized using FESEM and XRD. Optical characterizations were also performed on the ZnO SA. The SA exhibits broadband absorption from 1000 nm to 1600 nm, covering the S-band and C-band region. Using the balanced twin-detector technique, the SA has a saturation intensity of 0.016 $MWcm^{-2}$ and modulation depth of 3.5 %.

The ZnO SA was used in various cavities to obtain Q-switching in C- and S-band. Q-switched pulse in the C-band region was observed with repetition rate that increased from 42 kHz to 77 kHz while the pulse width reduced from 9.6 μs to 3.0 μs, as the pump power was increased. It has a maximum pulse energy of 48 nJ. The tunability of the SA was also investigated. Stable Q-switched pulse was observed as the lasing wavelength was varied from 1536 nm to 1586 nm, covering a broad tuning range of 50 nm.

In S-band regime, stable Q-switched pulse with peak wavelength at 1500 nm was observed using ZnO SA. As the pump power was increased, the repetition rate increased from 30 kHz to 48 kHz whereas the pulse width decreased from 5.4 μs to 2.3 μs. It has a low maximum pulse energy of 3.2 nJ, which is suitable for applications that require high repetition rate but low pulse energy. The tuning range of the saturable absorber in S-band was not as successful as the case in C-band. Q-switched pulse was observed but the corresponding SNR value of 27 dB is not sufficiently high to verify the stability of the pulse. The problem was attributed to the tunable bandpass filter with central wavelength of 1550 nm. By replacing the tunable bandpass filter with another one that operates in the S-band regime, might improve the quality of the Q-switched pulse.

All the results suggest that ZnO SA is a reliable saturable absorber for passive Q-switching in C- and S-band. This interesting material has huge potential to be exploited as saturable absorber and showed results comparable to conventional materials used as saturable absorbers. Moreover, laser in C-band is widely used in most optical communications whereas exploration into wavelength in S-band is also important to accommodate current heavy data traffic.

Future work based on zinc oxide saturable absorber can be further explored in L-band region to enable the creation of a wide-bandwidth pulsed fiber laser. Also, the possibility should not be limited to fiber laser only but also in solid state laser using mirrors. It would be interesting to compare the performance of ZnO SA in these two different types of laser configurations.

Furthermore, this work can be further extended to obtain supercontinuum using ZnO SA. Besides that, another possibility is to obtain narrower pulse and larger repetition rate through passive mode-locking using ZnO SA. Since ZnO has recovery time in the order of picoseconds, in theory, pulse width in the range of picoseconds can be achieved using ZnO SA.

The promising ability of ZnO as a saturable absorber also opened up opportunities to explore other metal oxides nanostructures as saturable absorber. This will increase the library of existing saturable absorbers and hopefully will expand our current knowledge and understanding about the physics of saturable absorbers.

REFERENCES

Ahmad, H., Ismail, M., Sathiyan, S., Reduan, S., Ruslan, N., Lee, C., Zulkifli, M., Thambiratnam, K., Ismail, M., & Harun, S. (2017). S-band Q-switched fiber laser using MoSe 2 saturable absorber. *Optics Communications, 382*, 93-98.

Ahmad, H., Reduan, S. A., Ali, Z. A., Ismail, M. A., Ruslan, N. E., Lee, C. S. J., Puteh, R., & Harun, S. W. (2016). C-Band Q-Switched Fiber Laser Using Titanium Dioxide (TiO_2) As Saturable Absorber. *IEEE Photonics Journal, 8*(1), 1-7.

Ahmad, H., Ruslan, N., Ismail, M., Ali, Z., Reduan, S., Lee, C., & Harun, S. (2016). Silver nanoparticle-film based saturable absorber for passively Q-switched erbium-doped fiber laser (EDFL) in ring cavity configuration. *Laser physics, 26*(9), 095103.

Ahmad, H., Ruslan, N. E., Ismail, M. A., Reduan, S. A., Lee, C. S. J., Sathiyan, S., Sivabalan, S., & Harun, S. W. (2016). Passively Q-switched erbium-doped fiber laser at C-band region based on WS_2 saturable absorber. *Applied Optics, 55*(5), 1001-1005.

Ahmad, H., Saat, N. K., & Harun, S. W. (2005). Effect of doped-fiber's spooling on performance of S-band EDFA. *Laser Physics Letters, 2*(8), 412.

Ahmad, H., Soltanian, M. R. K., Narimani, L., Amiri, I. S., Khodaei, A., & Harun, S. W. (2015). Tunable S-Band Q-Switched Fiber Laser Using Bi₂Se₃ as the Saturable Absorber. *IEEE Photonics Journal, 7*(3), 1-8.

Akhtar, M. J., Ahamed, M., Kumar, S., Khan, M. A. M., Ahmad, J., & Alrokayan, S. A. (2012). Zinc oxide nanoparticles selectively induce apoptosis in human cancer cells through reactive oxygen species. *International Journal of Nanomedicine, 7*, 845-857.

Antipov, O., Eranov, I., & Kositsyn, R. (2016). 36 W Q-switched Ho: YAG laser at 2097 nm pumped by a Tm fiber laser: evaluation of different Ho^{3+} doping concentrations. *Laser Physics Letters, 14*(1), 015002.

Arbore, M. A., Zhou, Y., Keaton, G., & Kane, T. (2002). *34dB gain at 1500nm in S-band EDFA with distributed ASE suppression.* Paper presented at the 2002 28TH European Conference on Optical Communication.

Bao, Q., Zhang, H., Ni, Z., Wang, Y., Polavarapu, L., Shen, Z., Xu, Q.-H., Tang, D., & Loh, K. P. (2010). Monolayer graphene as a saturable absorber in a mode-locked laser. *Nano Research, 4*(3), 297-307.

Bao, Q., Zhang, H., Ni, Z., Wang, Y., Polavarapu, L., Shen, Z., Xu, Q.-H., Tang, D., & Loh, K. P. (2011). Monolayer graphene as a saturable absorber in a mode-locked laser. *Nano Research, 4*(3), 297-307.

Becker, P. M., Olsson, A. A., & Simpson, J. R. (1999). *Erbium-doped fiber amplifiers: fundamentals and technology*: Elsevier.

Cao, G., & Wang, Y. (2004). *Nanostructures and nanomaterials: synthesis, properties, and applications*: World Scientific.

Chen, B., Zhang, X., Wu, K., Wang, H., Wang, J., & Chen, J. (2015). Q-switched fiber laser based on transition metal dichalcogenides MoS 2, MoSe 2, WS 2, and WSe 2. *Optics express, 23*(20), 26723-26737.

Chen, Y., Jiang, G., Chen, S., Guo, Z., Yu, X., Zhao, C., Zhang, H., Bao, Q., Wen, S., & Tang, D. (2015). Mechanically exfoliated black phosphorus as a new saturable absorber for both Q-switching and mode-locking laser operation. *Optics express, 23*(10), 12823-12833.

Chen, Y., Zhao, C., Chen, S., Du, J., Tang, P., Jiang, G., Zhang, H., Wen, S., & Tang, D. (2014). Large energy, wavelength widely tunable, topological insulator Q-switched erbium-doped fiber laser. *Selected Topics in Quantum Electronics, IEEE Journal of, 20*(5), 315-322.

Degnan, J. J. (1995). Optimization of passively Q-switched lasers. *Quantum Electronics, IEEE Journal of, 31*(11), 1890-1901.

El-Shall, M. S., Graiver, D., Pernisz, U., & Baraton, M. (1995). Synthesis and characterization of nanoscale zinc oxide particles: I. laser vaporization/condensation technique. *Nanostructured Materials, 6*(1-4), 297-300.

El-Sherif, A. F., & King, T. A. (2003). High-energy, high-brightness Q-switched Tm^{3+}-doped fiber laser using an electro-optic modulator. *Optics Communications, 218*(4), 337-344.

Garmire, E. (2000). Resonant optical nonlinearities in semiconductors. *IEEE Journal of Selected Topics in Quantum Electronics, 6*(6), 1094-1110.

Harun, S. W., Dimyati, K., Jayapalan, K. K., & Ahmad, H. (2007). An overview on S-band erbium-doped fiber amplifiers. *Laser Physics Letters, 4*(1), 10.

Hasan, M. Z., & Kane, C. L. (2010). Colloquium: Topological insulators. *Reviews of Modern Physics, 82*(4), 3045-3067.

Huang, Y., Luo, Z., Li, Y., Zhong, M., Xu, B., Che, K., Xu, H., Cai, Z., Peng, J., & Weng, J. (2014). Widely-tunable, passively Q-switched erbium-doped fiber laser with few-layer MoS_2 saturable absorber. *Optics express, 22*(21), 25258-25266.

Johnson, J. C., Knutsen, K. P., Yan, H., Law, M., Zhang, Y., Yang, P., & Saykally, R. J. (2004). Ultrafast carrier dynamics in single ZnO nanowire and nanoribbon lasers. *Nano Letters, 4*(2), 197-204.

Keller, U. (2003). Recent developments in compact ultrafast lasers. *Nature, 424*(6950), 831-838.

Keller, U. (2007). 2.1 Ultrafast solid-state lasers *Laser Physics and Applications* (pp. 33-167): Springer.

Keller, U., Weingarten, K. J., Kartner, F. X., Kopf, D., Braun, B., Jung, I. D., Fluck, R., Honninger, C., Matuschek, N., & Au, J. A. d. (1996). Semiconductor saturable absorber mirrors (SESAM's) for femtosecond to nanosecond pulse generation in solid-state lasers. *IEEE Journal of Selected Topics in Quantum Electronics, 2*(3), 435-453.

Kim, Y., Ahn, J., Kim, B. G., & Yee, D.-S. (2011). Terahertz birefringence in zinc oxide. *Japanese Journal of Applied Physics, 50*(3R), 030203.

Koechner, W. (2006). Mode-Locking *Solid-State Laser Engineering* (6th ed.). USA: Springer.

Li, H., Xia, H., Lan, C., Li, C., Zhang, X., Li, J., & Liu, Y. (2015). Passively-Switched Erbium-Doped Fiber Laser Based on Few-Layer MoS_2 Saturable Absorber. *Photonics Technology Letters, IEEE, 27*(1), 69-72.

Lin, J.-H., Chen, Y.-J., Lin, H.-Y., & Hsieh, W.-F. (2005). Two-photon resonance assisted huge nonlinear refraction and absorption in ZnO thin films. *Journal of applied physics, 97*(3), 033526.

Luo, Z., Huang, Y., Weng, J., Cheng, H., Lin, Z., Xu, B., Cai, Z., & Xu, H. (2013). 1.06 μm Q-switched ytterbium-doped fiber laser using few-layer topological insulator Bi 2 Se 3 as a saturable absorber. *Optics express, 21*(24), 29516-29522.

Martinez, A., & Sun, Z. (2013). Nanotube and graphene saturable absorbers for fibre lasers. *Nature Photonics, 7*(11), 842.

Mohanraj, J., Velmurugan, V., & Sivabalan, S. (2016). Transition metal dichalcogenides based saturable absorbers for pulsed laser technology. *Optical Materials, 60*, 601-617.

Novoselov, K. S., Geim, A. K., Morozov, S. V., Jiang, D., Zhang, Y., Dubonos, S. V., Grigorieva, I. V., & Firsov, A. A. (2004). Electric field effect in atomically thin carbon films. *science, 306*(5696), 666-669.

Paschotta, R. Q Switching. *Encyclopedia of Laser Physics and Technology.* Retrieved from https://www.rp-photonics.com/q_switching.html

Paschotta, R., Häring, R., Gini, E., Melchior, H., Keller, U., Offerhaus, H., & Richardson, D. (1999). Passively Q-switched 0.1-mJ fiber laser system at 1.53 μm. *Opt Lett, 24*(6), 388-390.

Petrov, G. I., Shcheslavskiy, V., Yakovlev, V. V., Ozerov, I., Chelnokov, E., & Marine, W. (2003). Efficient third-harmonic generation in a thin nanocrystalline film of ZnO. *Applied Physics Letters, 83*(19), 3993.

Popa, D., Sun, Z., Hasan, T., Torrisi, F., Wang, F., & Ferrari, A. C. (2011). Graphene Q-switched, tunable fiber laser. *Applied Physics Letters, 98*(7), 073106.

Scardaci, V., Sun, Z., Wang, F., Rozhin, A. G., Hasan, T., Hennrich, F., White, I. H., Milne, W. I., & Ferrari, A. C. (2008). Carbon nanotube polycarbonate composites for ultrafast lasers. *Advanced Materials, 20*(21), 4040-4043.

Snitzer, E., & Woodcock, R. (1965). Yb^{3+}–Er^{3+} GLASS LASER. *Applied Physics Letters, 6*(3), 45-46.

Sobon, G., Duzynska, A., Świniarski, M., Judek, J., Sotor, J., & Zdrojek, M. (2017). CNT-based saturable absorbers with scalable modulation depth for Thulium-doped fiber lasers operating at 1.9 µm. *Scientific Reports, 7*, 45491.

Soci, C., Zhang, A., Xiang, B., Dayeh, S. A., Aplin, D., Park, J., Bao, X., Lo, Y.-H., & Wang, D. (2007). ZnO nanowire UV photodetectors with high internal gain. *Nano Letters, 7*(4), 1003-1009.

Svelto, O. (2010). *Principles of Lasers*: Springer US.

Tran, V., Soklaski, R., Liang, Y., & Yang, L. (2014). Layer-controlled band gap and anisotropic excitons in few-layer black phosphorus. *Physical Review B, 89*(23), 235319.

Ümit, Ö., Hofstetter, D., & Morkoc, H. (2010). ZnO devices and applications: a review of current status and future prospects. *Proceedings of the IEEE, 98*(7), 1255-1268.

Wang, L., & Muhammed, M. (1999). Synthesis of zinc oxide nanoparticles with controlled morphology. *Journal of Materials Chemistry, 9*(11), 2871-2878.

Wang, Q. H., Kalantar-Zadeh, K., Kis, A., Coleman, J. N., & Strano, M. S. (2012). Electronics and optoelectronics of two-dimensional transition metal dichalcogenides. *Nat Nanotechnol, 7*(11), 699-712.

Wang, Z. L. (2004). Zinc oxide nanostructures: growth, properties and applications. *Journal of Physics: Condensed Matter, 16*(25), R829-R858.

Westin, G., & Nygren, M. (1992). On the formation of M^{2+}-Sb^{3+}-alkoxide precursors and sol-gel processing of M-Sb oxides with M= Cr, Mn, Fe, Co, Ni, Cu and Zn. *Journal of materials science, 27*(6), 1617-1625.

Woodward, R., & Kelleher, E. (2015). 2D Saturable Absorbers for Fibre Lasers. *Applied Sciences, 5*(4), 1440.

Woodward, R. I., Howe, R. C. T., Hu, G., Torrisi, F., Zhang, M., Hasan, T., & Kelleher, E. J. R. (2015). Few-layer MoS_2 saturable absorbers for short-pulse laser technology: current status and future perspectives [Invited]. *Photonics Research, 3*(2), A30.

Woodward, R. I., Howe, R. C. T., Runcorn, T. H., Hu, G., Torrisi, F., Kelleher, E. J. R., & Hasan, T. (2015). Wideband saturable absorption in few-layer molybdenum diselenide (MoSe2) for Q-switching Yb-, Er- and Tm-doped fiber lasers. *Optics express, 23*(15), 20051-20061.

Woodward, R. I., Kelleher, E. J., Howe, R. C., Hu, G., Torrisi, F., Hasan, T., Popov, S. V., & Taylor, J. R. (2014). Tunable Q-switched fiber laser based on saturable edge-state absorption in few-layer molybdenum disulfide (MoS(2)). *Opt Express, 22*(25), 31113-31122.

Yamashita, S. (2012). A Tutorial on Nonlinear Photonic Applications of Carbon Nanotube and Graphene. *Journal of Lightwave Technology, 30*(4), 427-447.

Yamashita, S., Inoue, Y., Maruyama, S., Murakami, Y., Yaguchi, H., Jablonski, M., & Set, S. (2004). Saturable absorbers incorporating carbon nanotubes directly synthesized onto substrates and fibers and their application to mode-locked fiber lasers. *Opt Lett, 29*(14), 1581-1583.

Yu, H., Zhang, H., Wang, Y., Zhao, C., Wang, B., Wen, S., Zhang, H., & Wang, J. (2013). Topological insulator as an optical modulator for pulsed solid-state lasers. *Laser & Photonics Reviews, 7*(6), L77-L83.

Zhou, D.-P., Wei, L., Dong, B., & Liu, W.-K. (2010). Tunable passively-switched erbium-doped fiber laser with carbon nanotubes as a saturable absorber. *Photonics Technology Letters, IEEE, 22*(1), 9-11.

Zulkifli, M., Jemangin, M., Harun, S., & Ahmad, H. (2011). Gain-flattened S-band depressed cladding erbium doped fiber amplifier with a flat bandwidth of 12 nm using a Tunable Mach-Zehnder Filter. *Laser physics, 21*(9), 1633-1637.

LIST OF PUBLICATIONS AND PAPERS PRESENTED

1) Ahmad, H., Lee, C., Ismail, M., Ali, Z., Reduan, S., Ruslan, N., . . . Harun, S. (2016). Zinc oxide (ZnO) nanoparticles as saturable absorber in passively Q-switched fiber laser. Optics Communications, 381, 72-76.

2) Ahmad, H., Lee, C. S. J., Ismail, M. A., Ali, Z. A., Reduan, S. A., Ruslan, N. E., & Harun, S. W. (2016). Tunable Q-switched fiber laser using zinc oxide nanoparticles as a saturable absorber. Applied Optics, 55(16), 4277-4281.